Article

Identification of the Ferri-Acinetobactin Outer Membrane Receptor in Aeromonas salmonicida subsp salmonicida and Structure-Activity Relationships of Synthetic Acinetobactin Analogues

Miguel Balado, Yuri Segade, Diego Rey, Carlos R Osorio, Jaime Rodriguez, Manuel L. Lemos, and Carlos Jiménez

ACS Chem. Biol., **Just Accepted Manuscript** • DOI: 10.1021/acschembio.6b00805 • Publication Date (Web): 12 Dec 2016

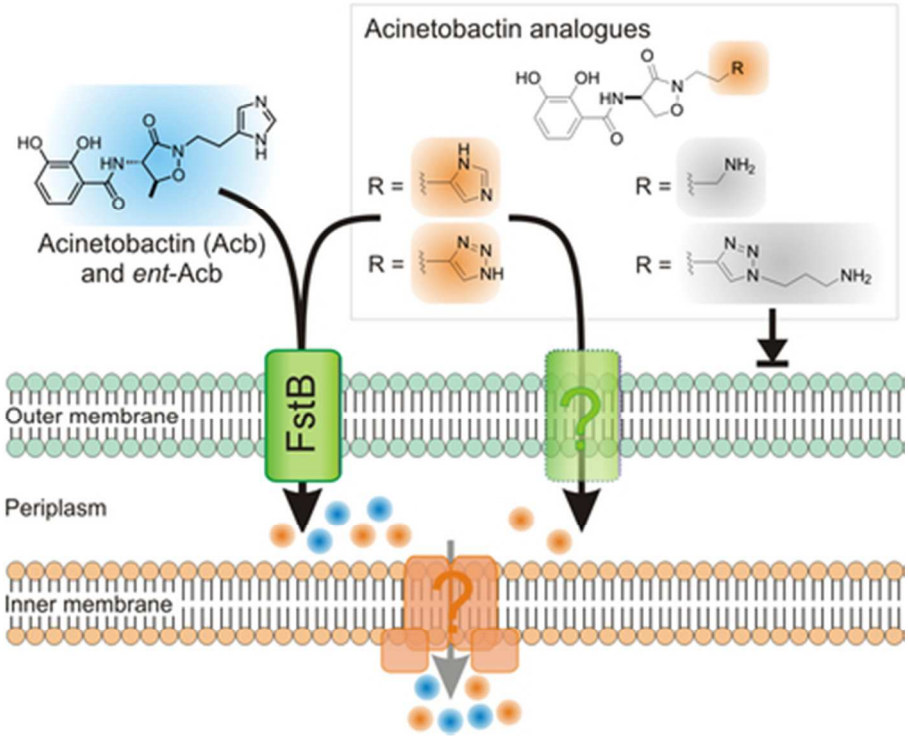

Graphical abstract

38x31mm (300 x 300 DPI)

Identification of the Ferri-Acinetobactin Outer Membrane Receptor in *Aeromonas salmonicida* subsp *salmonicida* and Structure-Activity Relationships of Synthetic Acinetobactin Analogues

Miguel Balado[‡], Yuri Segade[†], Diego Rey[‡], Carlos R. Osorio,[‡] Jaime Rodríguez[†*], Manuel L. Lemos,[‡*] and Carlos Jiménez[†*]

[†] *Centro de Investigacións Científicas Avanzadas (CICA), Departamento de Química Fundamental, Facultade de Ciencias, Universidade da Coruña, 15071 A Coruña, Spain*

[‡]. *Department of Microbiology and Parasitology, Institute of Aquaculture, Universidade de Santiago de Compostela, Campus Sur, Santiago de Compostela 15782, Spain*

*Corresponding author, E-mail: manuel.lemos@usc.es; jaime.rodriguez@udc.es; carlos.jimenez@udc.es

KEYWORDS: *Aeromonas*, *Aeromonas salmonicida*, furunculosis, iron uptake, siderophores, outer membrane siderophore receptors, acinetobactin, acinetobactin analogues

ABSTRACT

Aeromonas salmonicida subsp. *salmonicida*, the causative agent of furunculosis in several fish species, produces acinetobactin and amonabactin as siderophores. In a previous study we chemically characterized these siderophores and proposed a biosynthetic pathway based on genetic analysis. However, the internalization mechanisms of ferric-acinetobactin and ferric-amonabactin remain largely unknown. In the present study, we demonstrate that the outer membrane protein FstB is the ferric-acinetobactin receptor in *A. salmonicida* since an *fstB* defective mutant is unable to grow under iron limitation and does not use acinetobactin as an iron source. In order to study the effect that structural changes in acinetobactin have on its siderophore activity, a collection of acinetobactin-based analogues was synthesized, including its enantiomer and four demethylated derivatives. The biological activity of these analogues on an *fstB*(+) strain compared to an *fstB*(–) strain allowed structure-activity relationships to be elucidated. We found a lack of enantiomer preference on the siderophore activity of acinetobactin over *A. salmonicida* or on the molecular recognition by FstB protein receptor. In addition, it was observed that *A. salmonicida* could not use acinetobactin analogues when imidazole or a similar heterocyclic ring was absent from the structure. Surprisingly, removal of the methyl group at the isoxazolidinone ring induced a higher biological activity, thus suggesting alternative route(s) of entry into the cell that must be further investigated. It is proposed that some of the synthetic acinetobactin analogues described here could be used as starting points in the development of novel drugs against *A. salmonicida* and probably against other acinetobactin producers like the human pathogen *Acinetobacter baumannii*.

GRAPHICAL ABSTRACT

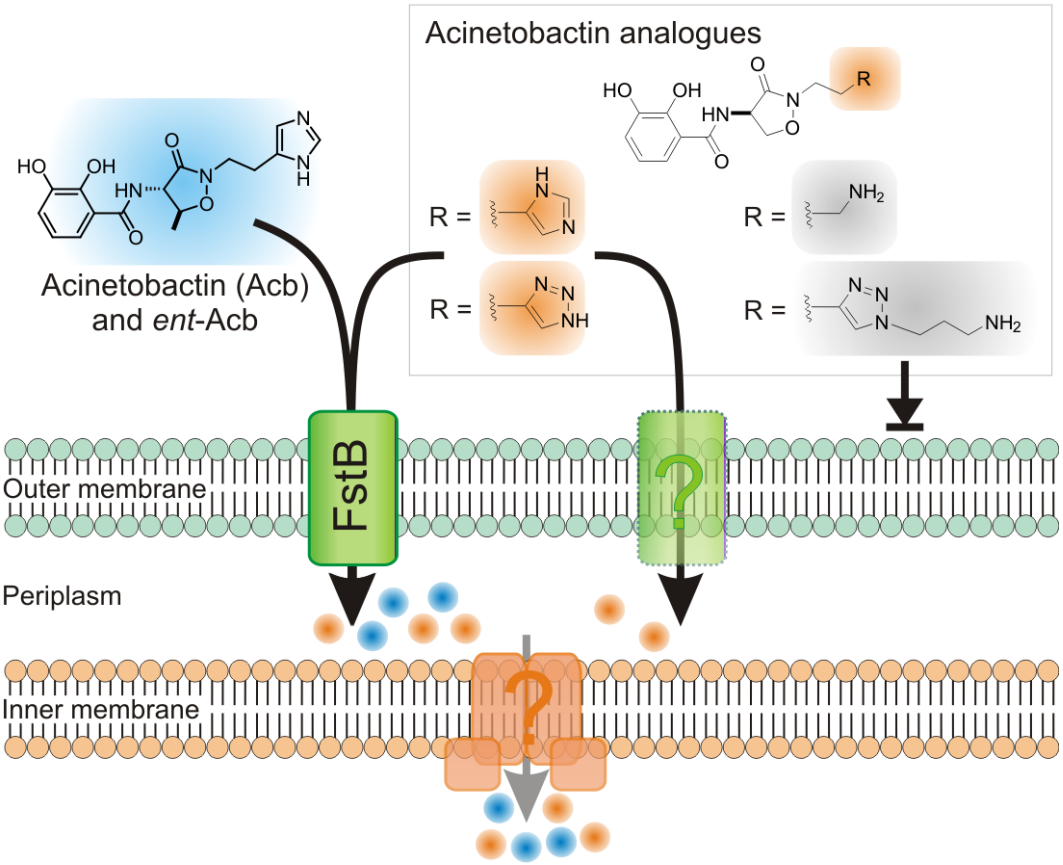

Iron is an essential trace nutrient for most organisms since it is a cofactor in key metabolic processes.[1] However, despite its high abundance in the Earth's crust, iron bioavailability is extremely low under aerobic conditions and at neutral pH because it is oxidized to insoluble ferric hydroxides.[2] In animal tissues iron is chelated by high-affinity iron-binding proteins that restrict its availability to microbial pathogens.[3] Therefore, most pathogenic bacteria have developed sophisticated mechanisms to obtain iron from host sources. These mechanisms are recognized as essential virulence factors for the survival of microbes within their hosts. Siderophore synthesis is a widespread iron uptake mechanism among bacterial pathogens. These compounds are low molecular weight, high affinity iron chelating molecules that are secreted by bacteria to acquire iron from their surroundings.[4] Siderophores are present in most pathogens and it has been shown that they are also important for the viability of marine bacteria in the natural environment.[5]

Aeromonas salmonicida subsp *salmonicida* (hereafter *A. salmonicida*) is a Gram-negative Gamma- proteobacterium that causes furunculosis, a devastating disease that affects salmonids and a variety of other non-salmonid fish, with a significant economic impact in the aquaculture industry worldwide.[6] In previous publications,[7] we reported that most *A. salmonicida* strains produce two catechol siderophores simultaneously: acinetobactin (Acb, **1a**), a siderophore first described in the human pathogen *Acinetobacter baumannii*,[8] and amonabactins such as amonabactin P750 (**2**), which were previously found in *Aeromonas hydrophila* (Figure 1).[9] While amonabactin genes are part of a gene cluster conserved in most *Aeromonas* species, acinetobactin synthesis is encoded by a second gene cluster only present in *A. salmonicida*. This cluster is phylogenetically more related to the cluster that encodes the siderophore pseudomonine in *Pseudomonas entomophila*[10] than to the cluster encoding Acb (**1a**) in *A. baumannii*.[11] Pseudomonine (**3**) and Acb (**1a**) only differ in the presence of the salicylic moiety in **3** rather than the catechol group in Acb (**1a**) (Figure 1). Most notably, the junction of the amonabactin cluster, which provides 2,3-dihydroxybenzoic acid (DHBA), and the likely horizontally acquired pseudomonine genes enable *A. salmonicida* to produce simultaneously amonabactin and acinetobactin.[7]

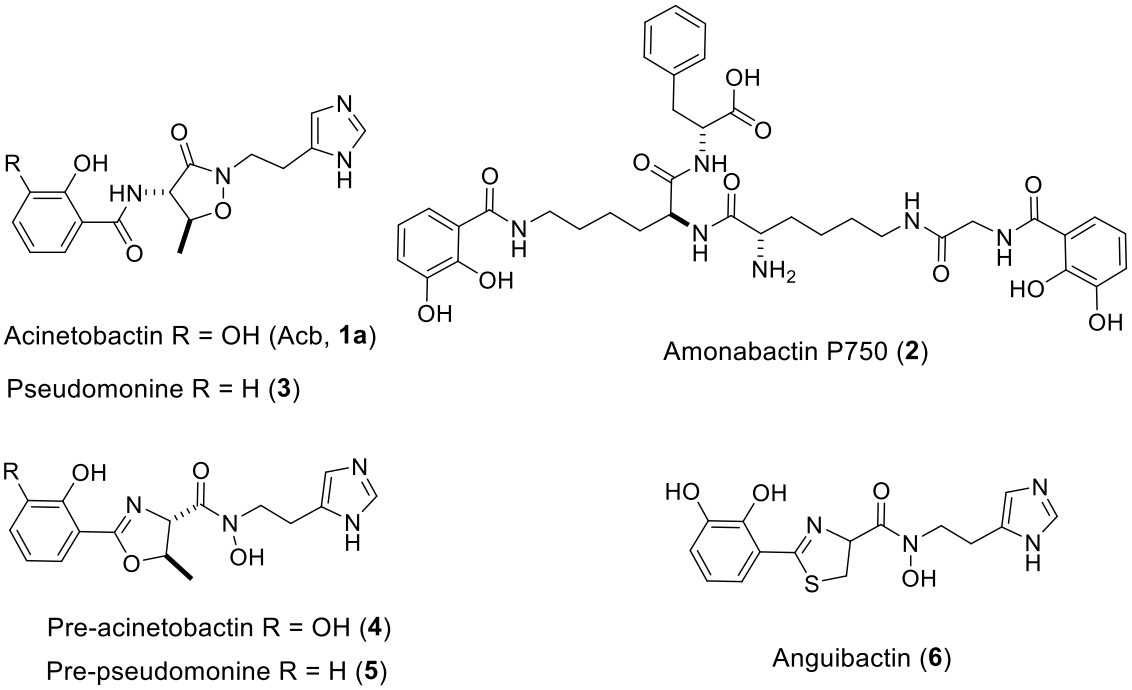

Figure 1. Structures of natural siderophores (**1**-**6**) isolated from different bacteria.

Once siderophores are synthesized and secreted outside the bacterial cells, they bind Fe^{3+} ions to form a ferric-siderophore complex. The ferric-siderophore is then internalized by the appropriate transport mechanism. In Gram-negative bacteria, ferric-siderophores are transported across the outer and inner membranes by an energy-dependent system. The components of such systems include a specific TonB-dependent ferric-siderophore transporter (TBDT) located in the outer membrane, coupled to an ABC transporter that catalyzes the final stages of ferric-siderophore transport through the cytoplasmic membrane from the periplasm to the cytosol. In this regard, nothing is known about the routes of entry of the ferric-siderophore complexes in *A. salmonicida*. It has been reported that three putative TBDT are specifically induced in *A. salmonicida* under iron deficiency and *in vivo* conditions.[12] One of these was initially named FstA but has subsequently been denoted as FstB in most recent studies due to the probable existence of two versions or alleles. FstA/B is a putative siderophore receptor that is present in virulent strains and it was used to develop PCR-based detection methods of *A. salmonicida*.[13,14] Thus, although *fstA/B* is a powerful molecular marker in the species, nothing is known about its biological function.

In the last decade, new antimicrobial agents have been developed using the 'Trojan horse' approach, which involves the synthesis of a novel compound from an

antibiotic linked to a siderophore that uses a specific siderophore route of entry into the cell.[15] This approach seeks to avoid microbial resistance, thus enhancing sensitivity and specificity.[16] In order to develop rationally designed Acb-derived antimicrobials, it is essential to know which TBDT serves as the entry route of ferric-Acb in *A. salmonicida* and to define the moieties of the siderophore that play a role in the receptor recognition.

In the study reported here, we demonstrated that the outer membrane receptor FstB is directly involved in the uptake of Acb (**1a**) in *A. salmonicida*. Furthermore, several synthetic analogues of Acb (**1a**) were prepared, including its enantiomer, and their capacity to serve as iron sources to *A. salmonicida* was evaluated. These analyses allowed us to establish very valuable structure-activity relationships that must be taken into consideration for the possible preparation of Acb-antibiotic conjugates.

RESULTS AND DISCUSSION

Sequence analysis of the acinetobactin genes of *A. salmonicida* revealed the existence of two candidate gene clusters that potentially encode ferric-siderophore uptake systems (Figure 2).[7,17] The first gene cluster could be related to a hydroxamate-type siderophore transport, being the closest homologue genes conserved in several bacterial genomes and annotated as *fhuABCDE*. Interestingly, FhuA shows homology to the putative ferrichrome receptor of *Aeromonas hydrophila* (FhuA, ac. Nº 4487379; 92% identity). The second cluster includes the uncharacterized *fstB* (encoding a TBDT) and genes for components of an ABC transporter (*asuBECDGF*). These show significant homology (between 43 to 79% aa identity) with the TBDT and ABC transporters involved in pseudomonine transport in *P. entomophila*[10] and acinetobactin uptake in *A. baumannii*.[11] Although FstB is homologous to the ferric pseudomonine receptor of *P. entomophila* (GenBank accession No CAK15297) and to the ferric acinetobactin receptor of *A. baumannii* (GenBank accession No YP_001713025), it only shares with those receptors 46 and 43% aa identity, respectively. Therefore, although a possible role of FhuA in ferric-siderophore acquisition cannot be ruled out, we hypothesize that *fstB* could encode the ferric-Acb TonB-dependent outer membrane receptor, which is indispensable for the ferric-siderophore internalization.

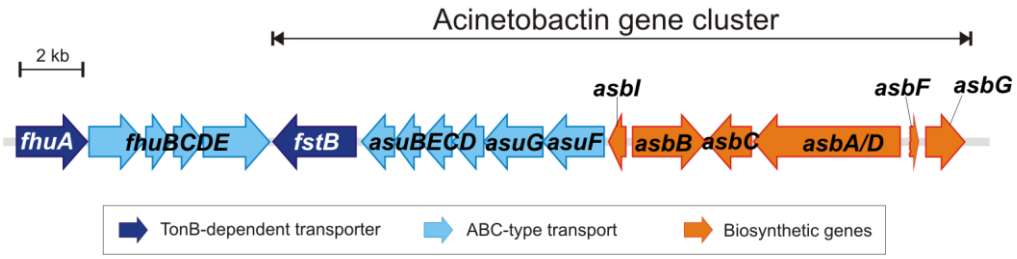

Figure 2. Scheme of the acinetobactin biosynthesis and transport gene cluster.[7]

fstB is essential for growth under iron starvation of *A. salmonicida* strains lacking amonabactin production

In order to assess the role of *fstB* and *fhuA* in ferric-acinetobactin transport, individual in-frame deletions were constructed by allelic exchange in strain RSP74.1. *A. salmonicida* RSP74.1 is a virulent strain that was previously used to characterize the *asb* genes.[18] It is a natural producer of Acb (**1a**) but it does not produce amonabactins (i.e. compound **2**)

due to a deletion in the *amoG* gene.[7]

When individual mutants were cultured under iron-sufficient conditions (CM9 plus 10 µM ferric sulfate), significant differences in growth levels were not observed with respect to the parental strain (Figure 3). However, under iron-restricted conditions (CM9 plus 75 µM 2,2'-dipyridyl), the Δ*fstB* mutant was severely affected in its ability to grow under iron starvation and it showed an equivalent phenotype to that of the mutant that is unable to produce Acb (**1a**) (RSP74.1Δ*asbD*). An analysis of the culture supernatants by the CAS assay showed similar levels of siderophore production in the Δ*fstB* mutant with respect to the parental strain (Figure 3). At an OD_{600} of approximately 1 in CM9 plus 50 µM 2,2'-dipyridyl, the parental strain and the mutant showed CAS values of ca. –0.38 (lower values indicate higher concentrations of siderophore).[19] This demonstrates that the growth phenotype of the Δ*fstB* mutant is not due to the lack of siderophore production. It is noteworthy that the RSP74.1Δ*fhuA* mutant is not affected in its ability to grow under iron-limiting conditions nor in its siderophore production (Figure 3). Complementation of the *fstB* mutation, by providing *in trans* an intact copy of the *fstB* gene, restored growth under iron limitation at the same level of wild type strain (Figure 3). Altogether, these results clearly indicate that the TBDT FstB is essential for RSP74.1 growth under iron deprivation and it must be directly involved in the utilization of Acb (**1a**) by *A. salmonicida*.

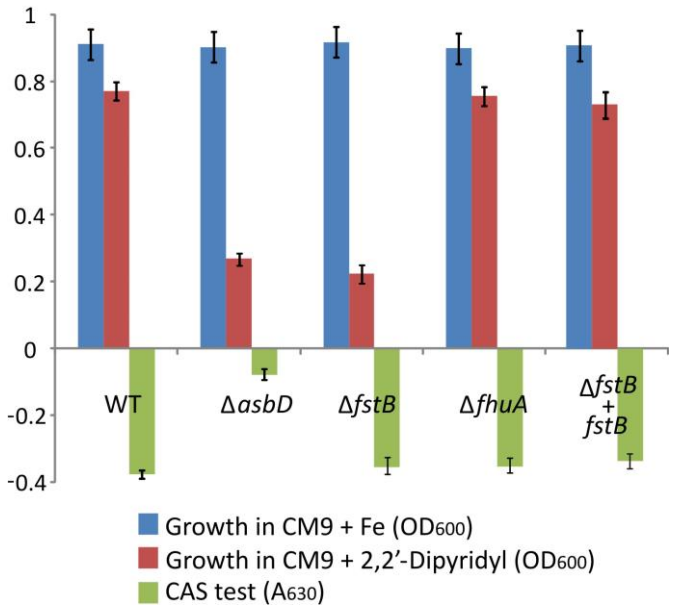

Figure 3. Growth (OD_{600}) after 12 h of incubation of *A. salmonicida* subsp *salmonicida* (RSP74.1 wild type, RSP74.1Δ*asbD*, RSP74.1Δ*fstB*, RSP74.1Δ*fhuA* and RSP74.1 Δ*fstB*

complemented with a wild type copy of the gene *fstB*) strains in CM9 minimal medium supplemented with $Fe_2(SO_4)_3$ (10 μM) or with addition of the iron chelator 2,2'-dipyridyl (75 μM).

fstB is the ferric-acinetobactin receptor in *A. salmonicida*

In order to demonstrate that FstB is the receptor for Acb (**1a**) in *A. salmonicida*, we first performed cross-feeding bioassays. *A. salmonicida* mutants RSP74.1Δ*asbD* and RSP74.1Δ*fstB* were used as indicator strains and *A. salmonicida* wild type strains RSP74.1 (produces Acb (**1a**) only) and VT45.1 (produces Acb (**1a**) and amonabactins (i.e. compound **217**) and *Acinetobacter baumannii* strain ATCC19606 (produces Acb (**1a**)) as test strains (Table S1). The results showed that all of the *A. salmonicida* and *A. baumannii* acinetobactin producer strains could promote growth of the Δ*asbD* mutant but not of the Δ*fstB* mutant (Table 1, Figure S1). However, *A. salmonicida* strains VT45.1 and VT45.1Δ*asbD* (a mutant that does not produce Acb (**1a**)) could promote growth of both mutants (Table 1, Figure S1) since they produce amonabactins, which can be utilized through its own receptor by all mutants, with its transport being independent of FstB.

To confirm the above results, we also tested the utilization of purified amonabactin P750 (**2**) and Acb (**1a**) by the indicator mutants. Amonabactin P750 (**2**) was used as an iron source by both mutants but the Δ*fstB* mutant was unable to utilize natural Acb (**1a**), although it could still use amonabactin P750 (**2**) (Table 1, Figure S1). As a comparison, a Δ*fhuA* mutant used Acb (**1a**) as efficiently as the parental strain (results not shown). These results reinforced the idea that *fstB* encodes the acinetobactin TBDT in *A. salmonicida* and they demonstrate that FstB is directly involved in the uptake of ferric Acb (**1a**).

Table 1. Results of cross-feeding experiments with two indicator strains.

	Ability to cross-feed	
	RSP74.1Δ*fstB*	**RSP74.1Δ*asbD***
Strains		
Aeromonas salmonicida subsp *salmonicida*		
RSP74.1 [a]	–	+
RSP74.1Δ*asbD* [b]	–	–
RSP74.1Δ*fstB* [a]	–	+
RSP74.1Δ*fhuA* [a]	–	+
VT45.1[a,c]	+	+
VT45.1Δ*asbD* [c]	+	+
Acinetobacter baumannii		
ATCC 19606 [a]	–	+
Pure natural siderophores		
Acb (**1a**)	–	+
Amonabactin P750 (**2**)	+	+

[a] Acinetobactin producer
[b] Does not produce any siderophore
[c] Amonabactin producer

fstB is the most abundant allele of the acinetobactin receptor gene in *A. salmonicida*

The first sequence of a ferric-siderophore transporter in *A. salmonicida* subsp. *salmonicida* was deposited in GenBank in 1995 and was named *fstA* (GI:1143382). Since then other versions (alleles) of this gene, which were called either *fstA* or *fstB*, have been sequenced and deposited in GenBank. The two alleles, *fstA* and *fstB*, have a nucleotide identity of 98% (Supporting Information, Figure S2); however, the protein similarity is only 86% due to the existence of certain regions that do not align to each other (Supporting Information, Figure S3). FstA and FstB show the characteristic TBDT domain architecture composed of a 22-stranded transmembrane β-barrel that encloses a globular plug domain. The N- and C-terminals are conserved among TBDTs so they are necessary for TonB interaction (N-terminal) and for the correct protein assembly in the outer membrane (C-terminal). In addition, the ligand binding site is usually located in the extracellular side of the plug domain.[20] The unmatched regions between FstA and FstB are located outside the most probable regions related to protein functionality. The differences in the amino acid sequences are mostly located in the extracellular loops and

outside the plug-domain and C- and N-terminals, so they should not affect protein function, although this possibility cannot be completely ruled out and must be further investigated.

Currently the distribution of *fstA/B* among *A. salmonicida* strains is unknown. A nested PCR test was used to detect *fstA*/*B* and differentiate between *fstA* or *fstB* alleles in a collection of 37 *A. salmonicida* strains isolated from diseased freshwater and marine fish. Interestingly, all *A. salmonicida* strains tested harbour the *fstB* version (results not shown). This result is consistent with the fact that only one of the 18 different *fstA/B* sequences deposited in GenBank corresponds to *fstA*.

Synthesis of Acb analogues (1b and 7–10)

The isolation and structure elucidation of Acb (**1a**), as the siderophore produced by *A. baumannii* ATCC19606, was reported in 1994.[8] However, it was suggested in 2009 that the reported structure **4** was an unstable intermediate, which was later named as pre-acinetobactin (Pre-Acb, **4**), and the correct structure was proposed as **1a**, which corresponds to an intramolecular nucleophilic substitution from **4** to **1a**.[21] A complete study about the acinetobactin isomerization at different pH was recently published.[22] The same type of rearrangement was previously observed in the natural analogue pseudomonine (**3**),[23] a blue-fluorescent siderophore, which was first isolated from *Pseudomonas fluorescens* AH2 obtained from Nile perch.[24] The structure of Acb as **1a**, including its absolute configuration, was confirmed by chemical synthesis.[25]

With the aim of elucidating some structure-activity relationships (SARs) in Acb (**1a**), analogues *ent*-acinetobactin (*ent*-Acb, **1b**) and four demethylacinetobactin derivatives (**7**–**10**) were prepared (Figure 4). The structural design of these derivatives was based on its simplicity in order to facilitate the preparation of conjugates to be used as chemical probes. Information from SARs could be very useful for the development of new antimicrobial strategies based on iron uptake mechanisms.

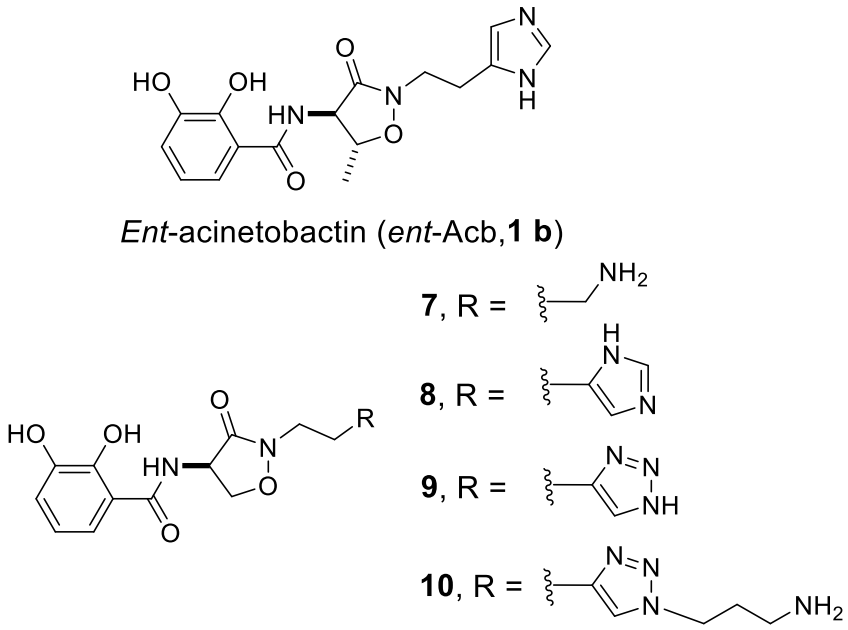

Figure 4. Structures of the synthetic acinetobactin analogues **1b** and **7**-**10**.

a) Synthesis of *ent*-Acb (1b)

In an effort to evaluate the influence of the stereochemistry of the chiral centres on the siderophore activity, we designed the synthesis of *ent*-Acb (**1b**) as shown in Scheme 1 based on the previous synthesis of Acb (**1a**) developed by Takeuchi *et al*.[25] .

Scheme 1. Synthesis of *ent*-Acb (1b) [a]

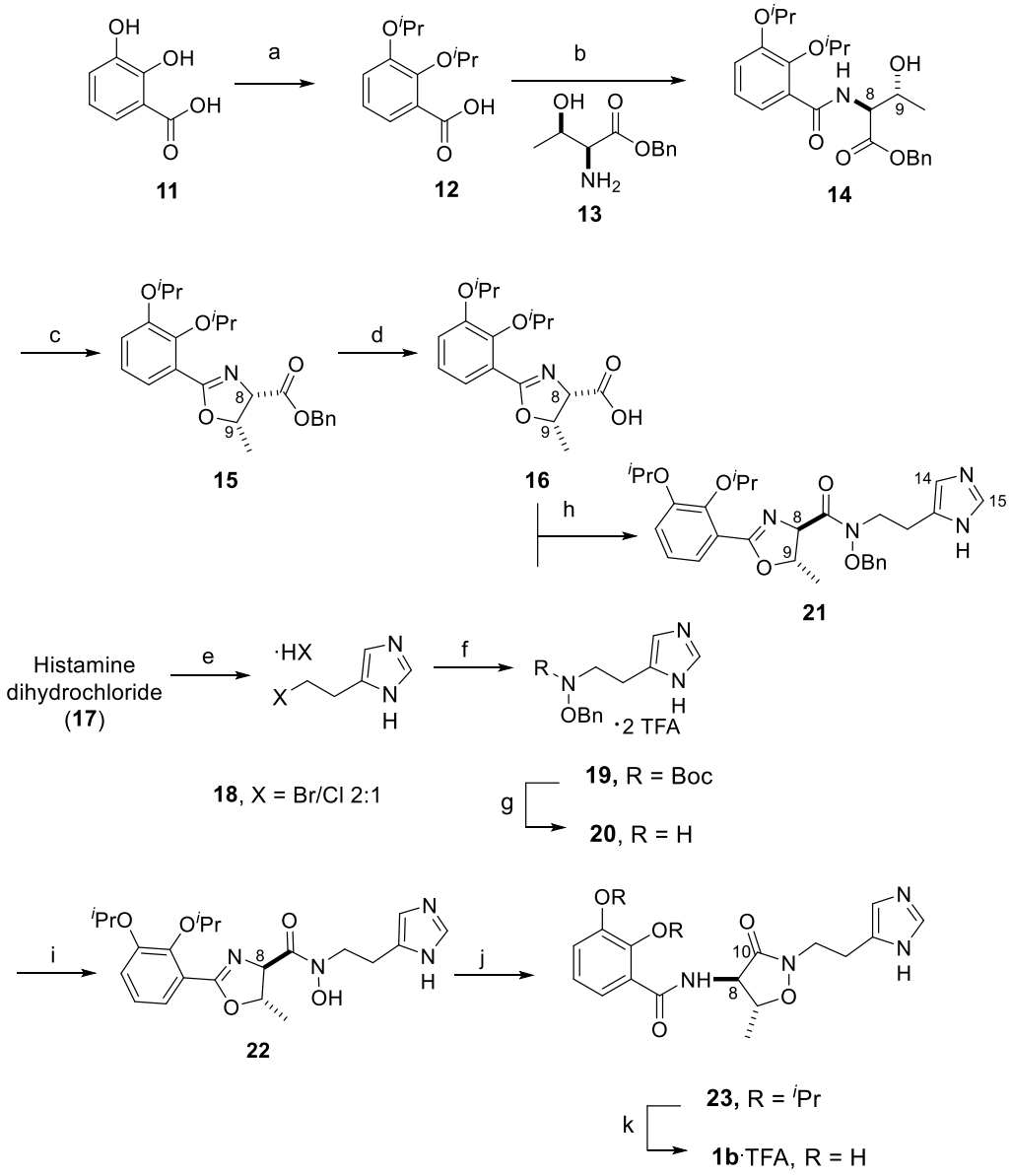

[a] *Reagents and conditions*:
(a) 1. ^{i}PrBr, K_2CO_3, KI, DMF, 50 ^{o}C (97%); 2. $Ba(OH)_2$, THF/H_2O, 50 ^{o}C (95%); (b) TBTU, Et_3N, DMF (64%); (c) $SOCl_2$, CH_2Cl_2 (93%); (d) H_2, Pd/C, MeOH (96%); (e) $NaNO_2$, H_2SO_4, KBr, -15 ^{o}C (90%); (f) NaH, BnONHBoc, DMF, 0 ^{o}C to r.t. (63%); (g) TFA/CH_2Cl_2 (1:4) (quant.); (h) CDI, DMF (69%); (i) H_2, Pd/C, MeOH (95%); (j) MeOH, Δ (87%); (k) BCl_3, CH_2Cl_2 -78 ^{o}C to -40 ^{o}C followed by HPLC purification (81%).

The synthesis was initiated with the access of a key amide **14**, which is easily obtained by the coupling of 2,3-diisopropyloxybenzoic acid (**12**)[26] with benzyl L-threonine (**13**).[27] The optimized conditions for this coupling to give the highest yield (64%) involved the use of 2.5 equivalents of Et_3N and TBTU as the coupling agent (instead of EDC or EDC/HOBt).[28]

Dehydrative-cyclization of amide **14** mediated by $SOCl_2$ in CH_2Cl_2 at room temperature gave the corresponding oxazoline **15**, which was debenzylated by hydrogenolysis to afford the carboxylic acid **16** in a very good yield in both steps (Scheme 1). Dehydrative-cyclization led to an inversion of configuration of the oxymethine carbon (C-9) in **15**, as supported by NOE cross peaks in **16** between protons H-8 and H-9 and confirming the *cis* disposition of these protons (see Supporting Information).

In parallel, the commercially available histamine dihydrochloride (**17**) was transformed into *O*-benzyloxyhistamine (**20**) *via* *N*-*tert*-butoxycarbonyl-*O*-benzyloxyamine (**19**) following the methodology described by Takeuchi *et al*.[25] (Scheme 1).

With these products in hand, oxazolinic acid **16** was coupled with *O*-benzyloxyhistamine (**20**) using EDC·HCl and HOBt to afford **21** in 43% yield. The yield could be improved to 69% when the reaction was performed with CDI in the absence of base. This coupling afforded the sterically stable *trans*-isomer **21** rather than the *cis*-isomer, probably due to epimerization of the activated acyl intermediate. The NOE cross peak between methyl group protons at C-9 and H-8 along with the lack of such correlation between protons H-8 and H-9 in the NOESY spectrum of **21** is consistent with the proposed *trans*-configuration (see the Supporting Information). A similar epimerization was also reported in the synthesis of another Acb analogue.[25] Debenzylation of **21** afforded the corresponding oxazoline **22** in very good yield and this was heated under reflux in MeOH to give the expected rearrangement of oxazoline **22** to isoxazolidinone **23**. This conversion was first observed from pre-pseudomonine (**5**) to pseudomonine (**4**)[23] and it confirms the electrophilic character of the oxazoline ring in **22**, which is intramolecularly attacked by the nucleophilic hydroxamate oxygen to give the isoxazolidinone ring in **23**. However this rearrangement does not occur in the case of the siderophore anguibactin (**6**) (Figure 1), which bears a thiazoline ring in **6** instead an oxazole ring in **3** and **5**, probably due to the decreased electrophilicity of C_β of the thiazoline ring relative to that of an oxazoline ring.[22]

Finally, removal of the isopropyl groups with BCl_3 in dry CH_2Cl_2 at low temperature afforded, after HPLC purification, *ent*-Acb (**1b**·TFA) in 23% global yield in 9 steps from 2,3-dihydroxy benzoic acid (Scheme 1).

Ent-Acb (**1b**·TFA) has the same NMR data and the same HPLC retention time as the natural TFA salt isolated from *A. salmonicida* subsp *salmonicida* Acb (**1a**·TFA). The absolute configuration of *ent*-Acb (**1b**·TFA) was confirmed by its circular dichroism (CD)

spectrum, which showed opposite Cotton effects, and a similar optical rotation, but with opposite signs, when compared Acb (**1a**·TFA) ($[\alpha]_D^{25}$ = +22 for **1b**·TFA instead of $[\alpha]_D^{25}$ = –29.7 for **1a**·TFA) (see the Supporting Information).

b) Synthesis of demethylacinetobactin analogues (7–10)

In order to compare the influence of the methyl group on the isoxazolidinone ring and the presence of similar heterocyclic rings such triazoles instead of imidazole on the siderophore activity of acinetobactin analogues, four demethylacinetobactin derivatives (compounds **7**–**10**) were prepared from a common intermediate **26** (Scheme 2). Compound **26** was synthesized from 2,3-dihydroxybenzoic acid (**11**), which was converted to **24**[29] and then coupled to the commercially available D-cycloserine (**25**) using an improved procedure employed by Walsh *et al*.[21]

The first demethyl Acb, compound **7**, was designed due to its simplicity and because it contains a primary amine group that may provide a possible anchor point for conjugation. Thus, the synthesis of **7** began with the *N*-alkylation of intermediate **26** with mesylate **27**, which was prepared in a straightforward manner from the commercially available 3-benzyloxycarbonylaminopropanol and methanesulfonyl chloride, to give compound **28**. The subsequent removal of Cbz and Bn protecting groups in **28** by hydrogenolysis afforded, after HPLC purification, **7**·TFA (Scheme 2).

Scheme 2. Synthesis of analogues 7 and 8[a]

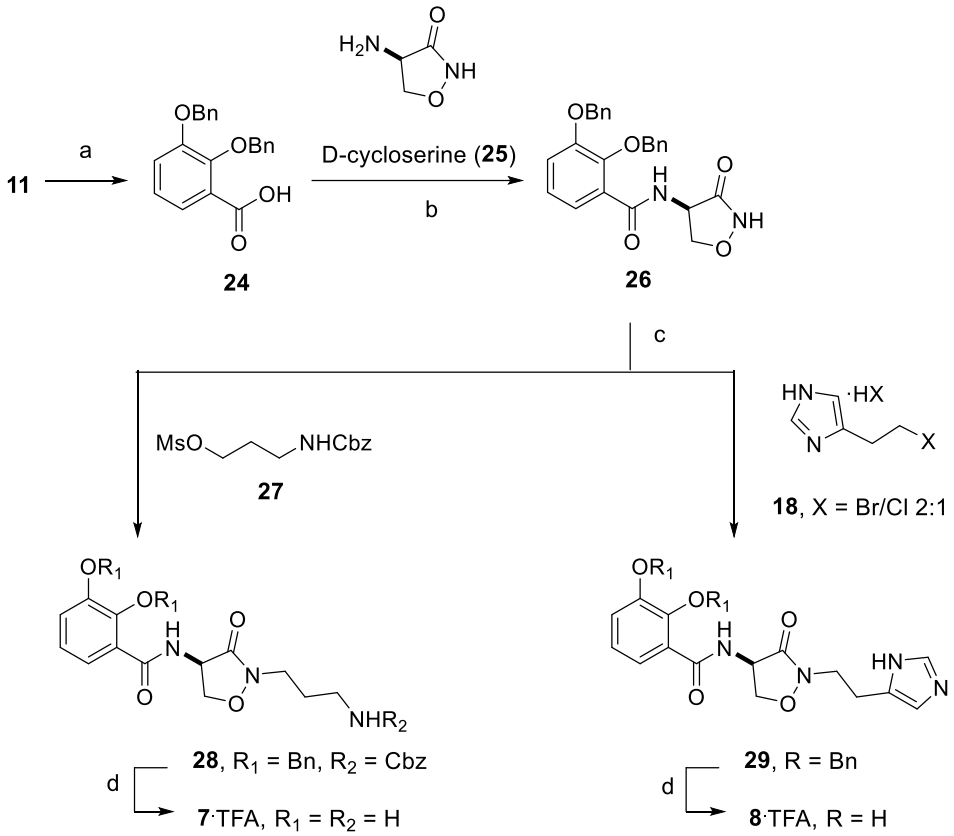

[a]*Reagents and conditions*: (a) 1. H_2SO_4, MeOH (95%); 2. BnBr, K_2CO_3, MeOH/$CHCl_3$ (quant.); 3. $Ba(OH)_2$, THF/H_2O, 50 °C (95%); (b) PyBroP, DIPEA, DMF/H_2O (45%); (c) Na_2CO_3, NaI, MeCN, 60 °C (56% for **29** and 65% for **30**); (d) H_2/Pd, AcOH:MeOH (1:4) followed by HPLC purification (85% for **7**·TFA and 99% for **8**·TFA).

The next demethylacinetobactin, compound **8**, was prepared following a procedure similar to that reported by Walsh *et al.*[21] *N*-Alkylation of the intermediate **26** with the substituted imidazole **18**, prepared previously for the synthesis of *ent*-Acb (**1b**), gave **29**, which was deprotected by hydrogenolysis and purified by HPLC to afford analogue **8**·TFA (Scheme 2).

A 'click-chemistry' reaction involving the efficient Cu(I)-catalyzed azide-alkyne couplings was used for the synthesis of the triazole analogues **9** and **10** (Scheme 3). This reaction is an extremely useful tool for preparation of conjugates.[30] Mesylate **30**, prepared from commercially available homopropargyl alcohol, was coupled with intermediate **26** using Na_2CO_3 and NaI to give compound **31**. Subsequent coupling of alkyne **31** with trimethysilyl azide in the presence of Cu(I)[31] furnished **32** in quantitative yield.

Subsequent debenzylation of **32** followed by purification by HPLC afforded the triazole analogue **9**·TFA (Scheme 3).

Scheme 3. Synthesis of analogues 9 and 10[a]

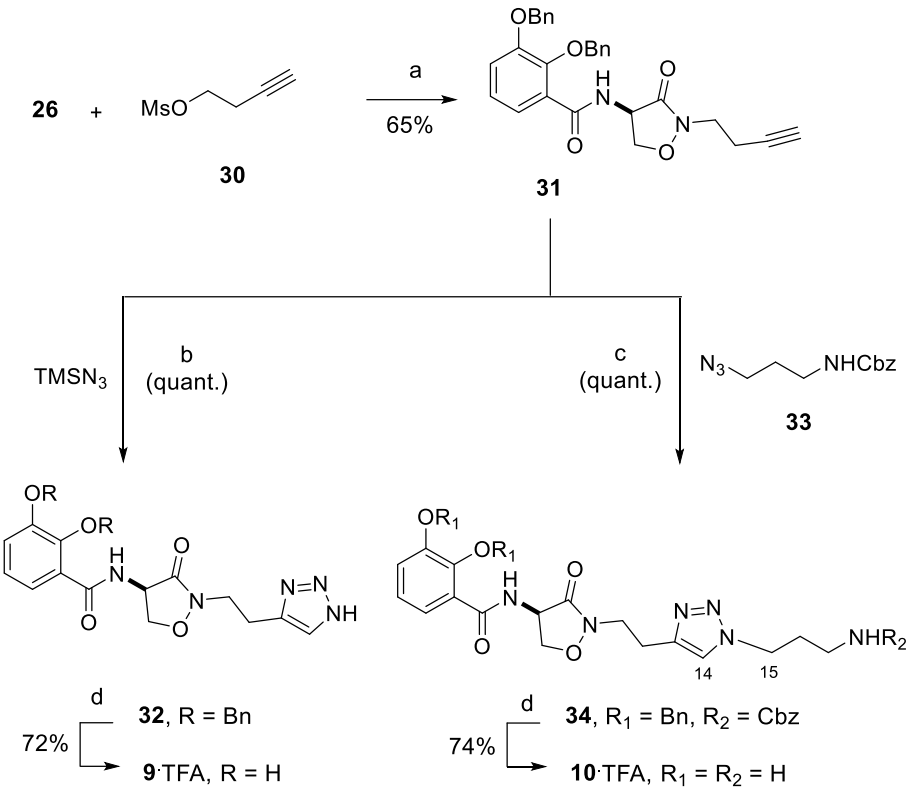

[a]*Reagents and conditions*:
(a) Na_2CO_3, NaI, MeCN, 60 °C (65%); (b) CuI, MeOH/DMF (1:9), 100 °C (quant.); (c) CuI, DIPEA, THF (quant.); (d) H_2/Pd, AcOH/MeOH (1:4) followed by HPLC purification (72% for **9**·TFA and 74% for **10**·TFA).

On the other hand, azide derivative **33**, prepared by displacement of the mesylate group in **30** with sodium azide, was coupled with alkyne **31** in a copper(I)-catalyzed 1,3-dipolar cycloaddition reaction following the procedure reported by Meldal *et al*.[32] In this way, the 1,4-substituted triazole **34** was obtained as the only regioisomer in quantitative yield. The regioselectively of the reaction was confirmed by the long range proton-carbon cross peak between the H-15 methylene protons at 4.32 ppm and the C-14 aromatic CH carbon at 126.1 ppm in the HMBC experiment on compound **34** (see Supporting Information). Debenzylation of the resulting product followed by HPLC purification afforded the desired triazole analogue **10**·TFA (Scheme 3).

Scheme 4. Alternative synthesis of intermediates 32 and 34 [a]

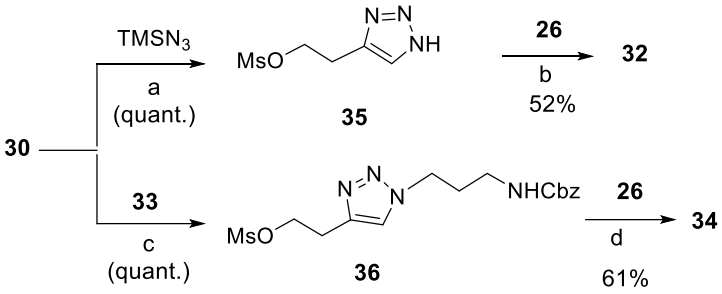

[a]*Reagents and conditions*:
(a) CuI, MeOH/DMF (1:9), 100 °C (quant.); (b) Na_2CO_3, NaI, MeCN, 60 °C (52%); (c) CuI, DIPEA, THF (quant.); (d) Na_2CO_3, NaI, MeCN, 60 °C (61%)

Alternatively, the triazole analogues **9** and **10** could be obtained by reversing the order of the reactions by preparing intermediates **35** and **36** as shown in Scheme 4. The number of reaction steps in both strategies is the same but the global yield was slightly lower on using the latter approach.

Biological evaluation of *ent*-Acb (1b) and demethyl-Acb analogues 7–10

In previous sections it was shown that *fstB* encodes the ferric-acinetobactin receptor in *A. salmonicida*. Moreover, several acinetobactin analogues were synthesized with the aim of studying the interaction between acinetobactin and its cognate receptor FstB. All these analogues showed CAS values indistinguishable from those of acinetobactin, which indicates that all them bind iron efficiently. In this section, the siderophore activity of all analogues was tested by growth promotion of an indicator strain *fstB*(+) in relation to an *fstB*(–) strain under iron-deficient conditions at physiological pH of 7.0.

a) Biological activity of *ent*-Acb (1b)

The results of growth promotion assays on natural Acb (**1a**) and its synthetic enantiomer *ent*-Acb (**1b**) against both *fstB*(+) and *fstB*(–) strains are shown in Figure 5 and Figure S4. The results show that *ent*-Acb (**1b**) promoted growth under iron-deficient conditions of the *fstB*(+) strain at the same level as Acb (**1a**) and in a dose-dependent manner (Figure 6). However, neither of these two compounds, Acb or *ent*-Acb, could promote the growth of the *fstB*(–) strain (Figure 5, Figure S4). This observation demonstrates not only that *ent*-Acb (**1b**) has siderophore activity but also that the FstB receptor (acinetobactin receptor) is the route of entry into the cell, thus confirming the results described above.

This observation reveals the lack of preference of the Acb enantiomer on the siderophore activity in *A. salmonicida* or on the molecular recognition by the FstB protein receptor. We previously found a similar lack of stereoisomeric influence of the amino acid scaffold on the siderophore activity in a series of analogues of vanchrobactin,[33] a siderophore isolated from *Vibrio anguillarum*.[34] These observations on Acb (**1a**) and vanchrobactin contrast those reported for enterobactin and pyochelin in relation to their corresponding enantiomers. *Ent*-enterobactin does not promote growth of *E. coli* K12 under iron-deficient conditions. Although *ent*-enterobactin binds to the outer membrane receptor FepA with similar affinity as enterobactin, however at a later stage, the Fes esterase, responsible for degrading the molecule, does not accept the *ent*-enterobactin or its iron complex as a substrate.[35] On the other hand, iron uptake and transcriptional regulation with pyochelin and *ent*-pyochelin are stereospecific processes in *Pseudomonas aeruginosa* and *P. fluorescens*, respectively. That stereospecificity is ensured not only by the outer membrane siderophore receptors but also by the cytosolic PchR regulators.[36] Indeed, the results obtained here help to expand our knowledge of the role of chirality in iron delivery.

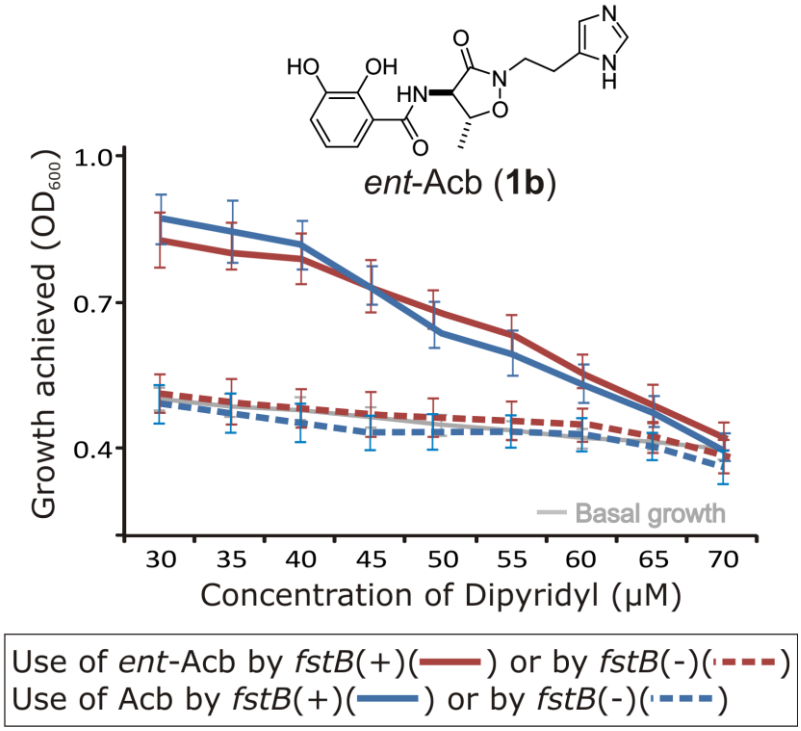

Figure 5. Biological activity of *ent*-Acb (**1b**) (blue lines) compared to Acb (**1a**) (brown lines). The graphs show the growth achieved after 12 h incubation in CM9 with different

concentrations of 2,2'-dipyridyl (from 30 to 70 µM). Indicator strains were an *fstB*(+) strain (RSP74.1Δ*asbD*) that is able to use Acb (**1b**) (Continuous lines) and an *fstB*(–) strain (RS74.1Δ*asbD*Δ*fstB*) that is unable to use Acb (**1b**) (dashed lines). The grey shaded area represents basal growth without addition of any siderophore.

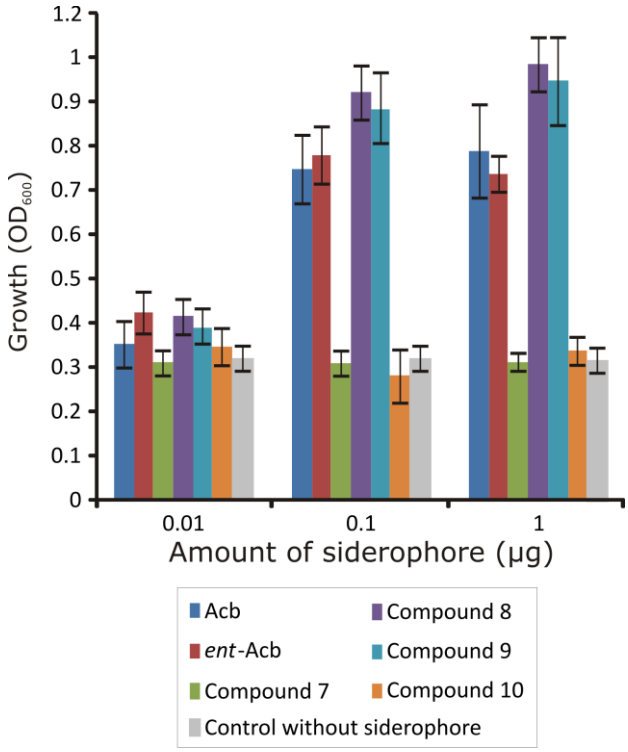

Figure 6. Growth achieved by *A. salmonicida fstB*(+) strain in CM9 medium with 40 µM dipyridyl supplemented with a 0.01, 0.1 and 1 µg of Acb (**1a**), *ent*-Acb (**1b**) or one of the analogues **7-10**.

b) Biological evaluation of demethylacinetobactin analogues 7–10

The biological activity of synthetic demethylacinetobactin analogues **7**–**10** was compared to the activity of natural Acb (**1a**) using growth promotion assays against *fstB*(+) (RSP74.1Δ*asbD*) and *fstB*(–) (RSP74.1Δ*asbD*Δ*fstB*) strains (Figure 7). When 1 µg of natural Acb (**1a**) was added to the *fstB*(+) strain cultures the maximum growth achieved was 1.4 (OD_{600}) at 40 µM 2,2'-dipyridyl, while under the same conditions the *fstB*(–) strain reached a maximum OD of only 0.55. This finding can be easily explained by the fact that this strain is unable to use Acb (**1a**) (see above).

The demethylacinetobactin analogues, compound **7** (bearing a propyl amino moiety instead of ethylimidazole group) and compound **10** (carrying a substituted

ethyltriazole ring), were almost unable to promote the growth of any of the indicator strains and hence they lack biological activity against both *fstB*(+) and *fstB*(–) strains (Figure 7, Figure S4). In contrast, the demethylacinetobactin analogues, compound **8** (bearing an imidazole ring) and compound **9** (bearing a triazole ring), were clearly able to promote the growth of the *fstB*(+) strain to a significantly higher extent than the natural Acb (**1a**), with a maximum OD of 1.6 (Figure 7, Figure S4) and a two-fold growth increase at 50 µM 2,2'-dipyridyl with respect to Acb (**1a**). Both compounds (**8** and **9**) promoted the growth of *A. salmonicida* in a dose-dependent manner (Figure 6). The use of these compounds (**8** and **9**) by the *fstB*(–) strain was analyzed and it was observed that, although their biological activity was lower in relation to the *fstB*(+) strain, they retained some growth promotion activity on the *fstB*(–) strain compared with Acb (**1a**). Compound **8** retained ca. 75% of the activity against the *fstB*(–) strain when compared to *fstB*(+) (OD_{600} = 1.2 vs. 1.5 at 45 µM 2,2'-dipyridyl) (Figure 7). This result suggests that compound **8** could mainly use a transporter alternative to the FstB receptor to enter into the cell. On the other hand, compound **9** also showed growth-promotion activity on the *fstB*(+) strain at about the same level as **8**, but the growth promotion on the *fstB*(–) strain was ca. 50% in relation to *fstB*(+) (OD_{600} = 0.7 vs. 1.5 at 45 µM 2,2'-dipyridyl) (Figure 7). This finding suggests that compound **9** must use both the FstB receptor and an alternative route of entry to be internalized. Further work is needed to identify this alternative transporter.

Additionally, the possibility that FhuA could participate in the uptake of compounds **8** and/or **9** was assessed by measuring the biological activity of these compounds in a strain that lacks FstB and FhuA (RSP74.1Δ*asbD*Δ*fstB*Δ*fhuA*) compared to an *fstB*(–) strain with an intact FhuA (RSP74.1Δ*asbD*Δ*fstB*). The results showed identical phenotypes for the two strains (data not shown) and this rules out FhuA as an alternative route of entry for compounds **8** and **9**.

In summary, all of the results discussed above suggest that the presence of an imidazole (**1a** and **8**), or a similar ring such as a triazole without substitution (**9**), is required to promote the growth of the *fstB*(+) indicator strain. Furthermore, the presence of a primary amino group (**7**) or a propylamino substituted triazole (**10**) makes the compound unable to promote growth since it does not serve as an iron source for *A. salmonicida*. The findings suggest that the recognition of acinetobactin by its cognate receptor FstB mostly resides in the presence of imidazole or a similar heterocyclic ring in its structure. Furthermore, the absence of the methyl group on the isoxazolidinone ring,

in combination with the presence of either an imidazole or a triazole ring (**8** and **9**), seems to open alternative route(s) of entry into the cell, which significantly increased the biological activity. This finding could be useful for the rational design of novel acinetobactin-based antimicrobials.

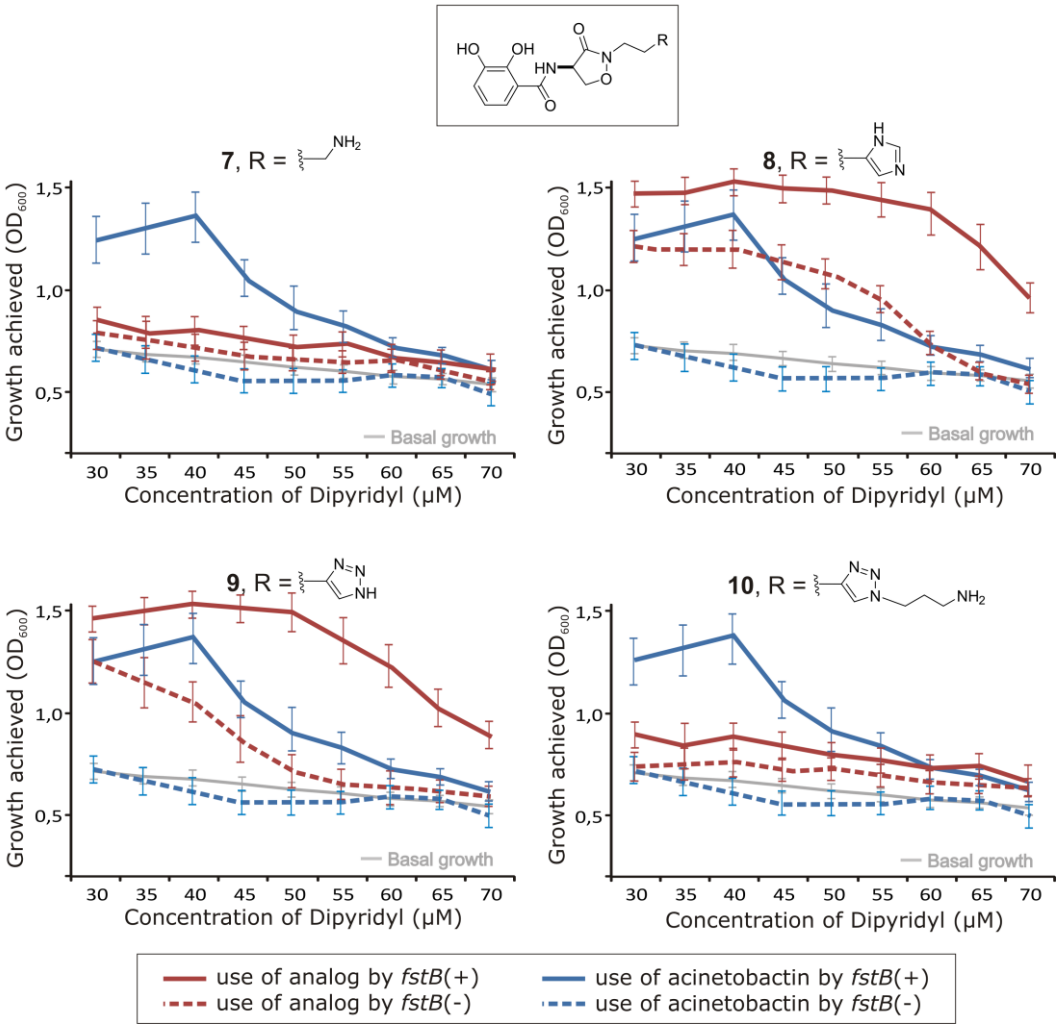

Figure 7. Biological activity results for Acb **1b** and analogues **7**–**10** (blue lines) compared to Acb (**1a**) (brown lines). The graphs show the growth achieved after 18 h of incubation in CM9 with different concentrations of 2,2'-dipyridyl (from 30 to 70 μM) with the addition of acinetobactin analogue (blue lines) compared to Acb (**1a**, brown lines). The indicator strains were an *fstB*(+) strain (RSP74.1Δ*asbD*) that is able to use Acb (**1a**) (continuous lines) and an *fstB*(–) strain (RS74.1Δ*asbD*Δ*fstB*) that is unable to use Acb (**1a**) (dashed lines). The grey shaded area represents basal growth without addition of any compound.

CONCLUSIONS

An understanding of the correlations between the structure and the chemical and biological activity of siderophores is crucial for the development of novel applications of the bacterial iron uptake mechanisms based on siderophores.[37] This information is very important, for instance, for the preparation of conjugates to be used as biosensors to study these mechanisms,[38] for the development of novel therapies against iron-overload related disease,[39] for the preparation of new antimicrobial agents that target bacterial pathways for the acquisition of iron, for a Trojan horse strategy to develop modified molecules with antimicrobial activity,[40] or for the synthesis of bioconjugates of siderophores to be tested as antibacterial vaccines.[41] In a recent study, we demonstrated that all virulent strains of the fish pathogen *A. salmonicida* produce acinetobactin as a siderophore.[7]

In the present study, by means of mutant construction, we identified the TonB-dependent outer membrane receptor necessary for the internalization of ferric-Acb and demonstrated that the *fstB* gene encodes this receptor. In order to establish some structure-activity relationships, several isoxazolidinone analogues of Acb were synthesized, including its enantiomer (*ent*- Acb), and their biological activity was evaluated by growth promotion assays on *fstB*(+) and *fstB*(–) strains. The observed lack of enantiomer preference on the recognition of Acb by FstB is worth highlighting. In addition, it seems that *A. salmonicida* cannot use Acb isoxazolidinone analogues if imidazole or a similar heterocyclic ring is not present in the structure. Surprisingly, removal of the methyl group at the isoxazolidinone ring leads to higher levels of biological activity, which suggests alternative route(s) of entry into the cell. More specifically, we suggest that compound **9** is a potential candidate as a vector in a Trojan horse strategy to develop new treatments against furunculosis in fish. Moreover, the fact that acinetobactin is also the main siderophore used by *Acinetobacter baumannii* opens the door to the development of novel drugs against this relevant human pathogen for which multi-drug-resistant (MDR) clinical isolates are frequently found.[42]

METHODS

A. Biological methods.

Bacterial Strains, Plasmids and Media. Strains and plasmids used, as well as those derived from this study are listed in Supplementary Information (Table S1). *A. salmonicida* subsp. *salmonicida* strains were grown at 25 ºC in Tryptic Soy Agar and Broth (Pronadisa) supplemented with 1% NaCl (TSA–1 and TSB–1, respectively), as well as in M9 minimal medium[43] (at physiological pH of 7.0) supplemented with 0.2% Casamino Acids (Difco) (CM9). *Escherichia coli* strains were routinely grown at 37 ºC in Luria Bertani (LB) medium (Pronadisa) or LB supplemented with the appropriate antibiotics. Ampicillin sodium salt (Ap) (Sigma–Aldrich) was used at 50 μg mL^{-1}; tetracycline (Tc), at 12 μg mL^{-1} and gentamicin (Gm) at 15 μg mL^{-1} (final concentrations). All stocks were filter sterilized and stored at –20ºC. The iron chelator 2,2´–dipyridyl (TCI) was dissolved in distilled water to prepare a stock solution at 20 mM that was added to the sterile media at appropriated concentrations.

DNA Manipulations and Bioinformatics Tools. Total genomic DNA from *A. salmonicida* was purified with the Easy–DNA kit (Invitrogen). Plasmid DNA purification and extraction of DNA from agarose gels were carried out using kits from Fermentas (Thermo–Fisher). PCR reactions were routinely carried out in a T–Gradient Thermal Cycler (Biometra), with *Taq* polymerase BioTaq (Bioline). FstA/B alignment were done with BLAST program.[44] SignalP 4.1 server was used to predict the presence and location of signal peptide cleavage site.[45] Domain content and prediction of the protein structures were done using Pfam protein families database[46] and SWISS-MODEL Server.[47] For FstB 3D structure modelling the crystal structure of Pyoverdine outer membrane receptor FpvA from *Pseudomonas aeruginosa* was used as template (SMTL id: 1xkh.1.).[48]

Detection of Acinetobactin Receptor *fstA* or *fstB* version. A nested PCR was designed to detect the suitable version of the acinetobactin receptor (*fstA* or *fstB*). External primer asbE_F and asbE_R were used to amplify *fstA/B* gene resulting in an amplicon of 1975 bp. One microliter of a 1/100 dilution in water of the first-round product was used as template for the second round using primers fstB_F and fstB_R that are specific of fstB version. Both PCR were done in a total volumen of 25 μl with *Taq* polymerase BioTaq (Bioline) according manufacture instructions. The cycling conditions were 95°C for 180 s, followed by 30 cycles of 94°C for 45 s, 57°C for 45 s, and 72°C for 90 s.

Construction of *fstB and fhuA* Mutants. In-frame deletions of *fstB* and *fhuA* in *A. salmonicida* subsp. *salmonicida* RSP74.1 were constructed by allelic exchange as previously described.[18] PCR amplifications of two fragments of each gene and flanking regions, when ligated together result in an in–frame (nonpolar) deletion. Primers used are listed in Supporting Information (Table S2). Each deleted gene construction was ligated into the suicide vector pKEK229.[49] The resulting plasmids were mated from *E. coli* S17-1-λ*pir*[50] into *A. salmonicida* subsp. *salmonicida* RSP74.1 wild type strain (Tc^R) and into previously constructed RSP74.1Δ*asbD* mutant strains,[18] and exconjugants with the plasmid (Ap^R) integrated in the chromosome by homologous recombination were selected. A second recombination event was obtained by selecting for sucrose (15%) resistance and further checking for plasmid loss and for allelic exchange. This process led to the generation of *A. salmonicida* subsp. *salmonicida* mutants RSP74.1Δ*fhuA*, RSP74.1Δ*fstB*, RSP74.1Δ*asbD*Δ*fstB* and RSP74.1Δ*asbD*Δ*fhu*A. Deletion of the parental gene was checked by DNA sequencing of the region involved to ensure that mutations were in-frame. For fstB gene complementation the ORF was PCR-amplified (primers listed in Supporting Information Table S3) with Hi-Fidelity Kapa Taq (Kapa), cloned into pHRP309 vector and mobilized from *E. coli* S17-1 ʎ-pir into the *A. salmonicida* R P74.1ΔfstB mutant.

Growth under Iron Limiting Conditions and Test of Siderophore Production. To test the ability of *A. salmonicida* subsp. *salmonicida* deleted mutants to grow under iron limiting conditions, overnight cultures in LB of the parental and mutant strains were adjusted to an optical density (OD_{600}) of 0.5 and diluted 1:100 in CM9 minimal medium containing the iron chelator 2,2´-dipyridyl at 75 µM. Cultures were incubated at 25 ºC with shaking at 150 rpm, and growth (OD_{600}) was measured after 12 h incubation. Siderophore production was measured using the chrome azurol-S (CAS) liquid assay,[19] which detects the presence of iron-chelating siderophore molecules. For siderophore production, strains were grown at 50 µM 2,2´-dipyridyl to allow enough growth to make siderophore secretion detectable. A non-inoculated CM9 sample containing 2,2´-dipyridyl at appropriate concentration and a sample from the *asbD* mutant were used respectively as spectrophotometric blank and as negative control for CAS liquid assay. Growth curves and CAS assays were carried out in triplicate, and results shown are the means of three independent experiments.

Cross-feeding Assays. Bioassays were designed to determine the role of the TBDTs FstB and FhuA in uptake of Acb (**1a**). Mutant strains RSP74.1Δ*asbD*, RSP74.1Δ*fhuA* and RSP74.1Δ*fstB* were used as indicator strains. They were inoculated into CM9 minimal medium containing the iron chelator 2,2´-dipyridyl at 150 µM, a concentration higher than the MIC for the wild type strain. *A. salmonicida* wild type strains RSP74.1 (produces only Acb (**1a**)) and VT45.1 (produces Acb (**1a**) and amonabactin) and *Acinetobacter baumannii* strain ATCC 19606 (produces Acb (**1a**)) were cultured on LB agar plates, cells were harvested with a sterile loop and placed on top of the indicator strain plates. Purified Acb (**1a**) and amonabactin P750 (**2a**), were deposited on the plates surface in paper discs (6 mm diameter) containing 25 µg of each siderophore. The results were scored as positive when a growth halo of the indicator strains was visible around discs. A disc containing 10 µl of a solution of $Fe_2(SO_4)_3$ 10 µM was used as positive growth control.

Quantification of the Biological Activity of *ent*-Acinetobactin and Compounds 7-10. The potential of *ent*-Acb (**1b**) and Acb analogues (compounds **7**-**10**) to promote the growth of *A. salmonicida* was compared to natural Acb (**1a**). As indicators of the biological activity, we used a *fstB*(+) strain and a *fstB*(-) strain that were cultured under increasing iron-deficient conditions (concentration of 2,2'-dipyridyl from 30 to 70 µM). As *fstB*(+), we used the mutant strain RSP74.1Δ*asbD* that is able to efficiently acquire acinetobactin although cannot produce it (Figure 7). As *fstB*(-) strain, we used the double mutant RSP74.1Δ*asbD*Δ*fstB* that is unable to produce or transport acinetobactin. Both *fstB*(+) and *fstB*(-) strains showed identical MIC of 2,2'-dipyridyl (ca. 35 µM), which is significantly lower than that of RSP74.1 wild type (around 100 µM). The addition to the culture medium of an *Acb* analogue that can be used as iron source by these indicator strains will promote their growth and will increase the MIC of 2,2'-dipyridyl. Consequently, we assumed that the maximum growth achieved (OD_{600}) by each strain will be related to the biological activity of the compounds tested.

Mid-log-phase *A. salmonicida* cultures of both indicators (*fstB*(+) and *fstB*(-)) in TSB-1 were adjusted to an OD_{600}=0.5 and diluted 1/20 in CM9 (at physiological pH of 7.0) containing increasing inhibitory concentrations of 2,2'-dipyridyl, from 30 and 70 µM. Growth promotion assays were performed using 96-well microtiter plates. Each well contained 100 µl of CM9, supplemented with the appropriated concentration of 2,2'-dipyridyl, inoculated with the indicator strain. One µg of the compound to be tested, either

natural Acb (**1a**), *ent*-Acb (**1b**) or some of the Acb analogues **7**-**10**, was added to each plate well, giving final concentrations of 2.9 µM for Acb and *ent*-Acb; 3.0 µM for compounds **8** and **9**; 3.4 µM for compound **7** and 2.6 µM for compound **10**. The plates were incubated for 18 h at 25 ºC under agitation at 150 rpm, and the growth achieved was evaluated by measuring the OD_{600} with an Infinite 200 PRO (TECAN) microplate reader. In the case of *ent*-Acb (**1b**) it was measured after 12 h. Each sample was duplicated within each plate and the assays were repeated three times. All the replicas showed similar results. *N*egative controls were made with the no addition of Acb (**1a**) (or any of the compound tested), and a plate well with non-inoculated CM9 was used as spectrophotometric blank. Mean and standard deviation were calculated for each measure.

B) Chemistry Methods

General information and procedures. Nuclear magnetic resonance spectra (proton and carbon) were recorded on Bruker AC200 F, and 300 or 500 Advance spectrometers at the University of A Coruña, using $CDCl_3$, D_2O and CD_3OD as the solvents and internal standards. Multiplicities of ^{13}C signals were obtained by DEPT. Medium-pressure chromatographic separations were carried out on silica gel 60 (230–400 mesh). Optical rotations were determined on a JASCO DIP-1000 polarimeter, with Na (589 nm) lamp and filter. LREIMS and HRESIMS were measured on Applied Biosystems QSTAR Elite. HPLC separations were carried out on an Agilent HP1100 liquid chromatography system equipped with a solvent degasser, quaternary pump and an UV detector (Agilent Technologies, Waldbronn, Germany). In the HPLC separations a Discovery® column HS F5 (100x4.6 mm, 5 µm) and an Eclipse® column XDB-C18 (150x4.6 mm, 5 µm) were used.

All moisture-sensitive reactions were carried out under an atmosphere of argon in flame-dried glassware closed by rubber septum, unless otherwise noted. Solvents were distilled prior to use under argon atmosphere and dried according to standard procedures using the following desiccants: Na/benzophenone for THF and Et_2O; CaH_2 for dichloromethane, pyridine and triethylamine; magnesium for methanol and anhydrous $CaSO_4$ for acetone. DMF was distilled over CaH_2 and was kept over molecular Sieves 4Å under argon atmosphere. Solutions and solvents were added via syringe or cannula. Thin layer chromatography was performed using silica gel GF-254 Merck, spots were revealed employing UV light (254 nm) and/or by heating the plate pre-treated with an ethanolic

solution of phosphomolibdic acid, a solution of cerium sulphate or a solution of ninhydrine in BuOH-AcOH-H2O. CRYOCOOL apparatus was used for low-temperature reactions. Abbreviations for the reagents used in the synthesis: TBTU: O-(Benzotriazol-1-yl)-N,N,N′, N′-tetramethyluronium tetrafluoroborate; EDC: N-(3-Dimethylamino-propyl)-N′-ethylcarbodiimide hydrochloride; HOBt 1-Hydroxybenzotriazole; CDI: 1,1′-Carbonyldiimidazole.

Experimental Procedures and Physical Data of Compounds

Synthesis of acinetobatin analogue *ent*-Acb (1b)

Compound 14.- To a stirrer solution of acid **12** (1.00 g, 4.21 mmol) in DMF (20 mL) was added amine **13** (0.80 g, 3.82 mmol), TBTU (0.80 g, 3.82 mmol) and Et_3N (1.33 mL, 9.55 mmol), at room temperature overnight. The mixture was diluted with EtOAc (50 mL) and washed with $NaHCO_3$ saturated aqueous solution, water, citric acid (0.1 M), water and brine. The organic layer was dried over anhydrous $MgSO_4$ and filtered, the solvent was removed under reduced pressure. The crude was purified by silica gel chromatography (hexane/EtOAc, 4:1), affording compound **14** as an amorphous solid (1.49 g, 64%). ^{1}H NMR (300 MHz, $CDCl_3$): δ_H = 8.94 (d, *J* = 8.3 Hz, 1H, NH); 7.73 (dd, *J* = 7.5, 2.1 Hz, 1H, H-6); 7.44-7.29 (m, 5H); 7.14-6.97 (m, 2H, H-4/H-5); 5.23 (s, 2H, –OC$\underline{H_2}$Ph); 4.95-4.74 (m, 1H,–OC$\underline{H}$Me$_2$); 4.95-4.74 (m, 1H, H-8); 4.57 (hept, *J* = 6.1 Hz, 1H, –OC$\underline{H}$Me$_2$); 4.48-4.31 (m, 1H, H-9); 1.42-1.31 (m, 9H, –OCH$\underline{Me_2}$ & Me); 1.32-1.19 (m, 6H, –OCH$\underline{Me_2}$). ^{13}C NMR (75 MHz, $CDCl_3$): δ_C = 170.9 (CO, C-7); 166.3 (CO, C-10); 150.8 (C, C-2); 146.7 (C, C-3); 135.3 (C); 128.6 (CH); 128.4 (CH); 128.3 (CH); 127.3 (C, C-1); 123.4 (CH, C-4); 123.3 (CH, C-5); 119.3 (CH, C-6); 71.3 (CH, –O$\underline{C}$HMe$_2$); 68.5 (CH, –O$\underline{C}$HMe$_2$); 67.1 (CH, C-9); 58.1 (CH, C-8); 22.1 (CH_3, Me); 22.0 (CH_3, –OCH$\underline{Me_2}$); 21.5 (CH_3, –OCH$\underline{Me_2}$); 20.1 (CH_3, –OCH$\underline{Me_2}$). HRMS (ESI+): calcd for $C_{24}H_{31}NO_6Na$ $[M+Na]^+$ 452.2043, found 452.2041. $[\alpha]_D^{25}$ = +27.3 (c = 0.52, $CHCl_3$).

Compound 15.- $SOCl_2$ (0.74 mL, 10.12 mmol) was added dropwise over a previously prepared solution of compound **14** (0.72 g, 1.68 mmol) in CH_2Cl_2 (20 mL), cooled at 0 ºC. The reaction was allowed to reach room temperature and then, it was stirred overnight. The reaction flask was placed on a water with ice bath and it was neutralized pouring a saturated solution of $NaHCO_3$ dropwise. After extraction with CH_2Cl_2 (3 x 50 mL), the combined organic layers were dried over anhydrous $MgSO_4$, filtered and the solvent

removed under reduced pressure. The crude was purified by silica gel chromatography (hexane/EtOAc, 3:1) affording compound **15** as a dark orange oil (0.64 g, 93%). ^{1}H NMR (300 MHz, $CDCl_3$): δ_H = 7.40-7.32 (m, 6H); 7.05-6.94 (m, 2H, H-4/H-5); 5.28-5.15 (m, 2H, OC$\underline{H}_2$Ph); 5.08-4.88 (m, 2H, H8/H9); 4.52 (dhept, *J* = 8.6, 6.1 Hz, 2H, ,–OC$\underline{H}$Me$_2$); 1.34 (d, *J* = 6.1 Hz, 3H, Me); 1.31 (d, *J* = 6.2 Hz, 3H, –OCH$\underline{Me}_2$); 1.30 (d, *J* = 6.2 Hz, 3H, –OCH$\underline{Me}_2$); 1.23 (d, *J* = 6.2 Hz, 3H, –OCH$\underline{Me}_2$), 1.22 (d, *J* = 6.2 Hz, 3H, –OCH$\underline{Me}_2$). ^{13}C NMR (75 MHz, $CDCl_3$): δ_C = 169.8 (CO, C-7); 166.3 (C, C-10); 151.7 (C, C-2); 148.2 (C, C-3); 135.3 (C); 128.7 (CH); 128.5 (CH); 128.4 (CH); 123.8 (C, C-1); 123.5 (CH, C-4); 123.2 (CH, C-5); 120.2 (CH, C-6); 77.7 (CH, C-9); 75.9 (CH, –O$\underline{C}$HMe$_2$); 71.7 (CH, ,–O$\underline{C}$HMe$_2$); 71.5 (CH, C-8); 66.8 (CH_2, –OC$\underline{H}_2$Ph); 22.3 (CH_3, –OCH$\underline{Me}_2$); 22.1 (CH_3, –OCH$\underline{Me}_2$); 16.1 (CH_3, Me). HRMS (ESI+) calcd for $C_{24}H_{30}NO_5$ $[M+H]^+$ 412.2118, found 412.2132. $[\alpha]_D^{23}$ = +59.5 (c = 0.95, $CHCl_3$).

Compound 16.- A suspension of compound **15** (0.55 g, 1.28 mmol) and palladium on charcoal 5% (50 mg) in MeOH (25 mL) was stirred at room temperature under H_2 atmosphere (1 atm) during 2 hours. After this time, the solution was filtered through Celite and the solvent was removed under reduced pressure, affording compound **16** as a greyish solid (0.39, 96%). ^{1}H NMR (500 MHz, CD_3OD), δ_H (ppm): 7.33 (dd, *J* = 7.8, 1.6 Hz, 1H, H-6); 7.21 (dd, *J* = 8.3, 1.5 Hz, 1H, H-4); 7.12 (t, *J* = 8.0 Hz, 1H, H-5); 5.67 (qd, *J* = 6.7, 3.1 Hz, 1H, H-9); 4.66 (hept, *J* = 6.0 Hz, 1H, –OC$\underline{H}$Me$_2$), 4.58 (hept, *J* = 6.0 Hz, 1H, –OC$\underline{H}$Me$_2$); 3.94 (d, *J* = 3.1 Hz, 1H, H-8); 1.45 (d, *J* = 6.7 Hz, 3H, Me); 1.36 (d, *J* = 6.0 Hz, 6H, –OCH$\underline{Me}_2$); 1.28 (d, *J* = 6.0 Hz, 3H, –OCH$\underline{Me}_2$), 1.27 (d, *J* = 6.0 Hz, 3H, –OCH$\underline{Me}_2$). ^{13}C NMR (75 MHz, CD_3OD), δ_C (ppm): 170.7 (CO, C-10); 167.9 (C, C-7); 151.3 (C, C-2); 148.0 (C, C-3); 123.3 (C, C-4); 122.1 (CH, C-5); 120.1 (CH, C-6); 118.9 (C, C-1); 80.2 (CH, C-9); 76.3 (CH, –O$\underline{C}$HMe$_2$); 71.1 (CH, –O$\underline{C}$HMe$_2$); 68.7 (CH, C-8); 21.3 (CH_3, –OCH$\underline{Me}_2$); 21.1 (CH_3, –OCH$\underline{Me}_2$); 20.9 (CH_3, –OCH$\underline{Me}_2$); 20.8 (CH_3, –OCH$\underline{Me}_2$); 15.1 (CH_3, Me). HRMS (ESI+) calcd for $C_{17}H_{24}NO_5$ $[M+H]^+$ 322.1648, found 322.1666. $[\alpha]_D^{24}$ = +19.5 (c = 0.62, CH_3OH).

Compound 19.- Over a cooled (0 ºC) solution of *tert*-butyl *N*-(benzyloxy)carbamate (0.76 g, 3.42 mmol) in dry DMF (25 mL) was added NaH in two portions (0.34 g, 13.41 mmol). It was allowed to reach room temperature and stirred during 30 min. Afterwards, 4(5)-(2-haloethyl)imidazole hydrochloride (**18**)[51] was added (0.60 g, 2.85 mmol) and the reaction was kept at 50 ºC overnight. After this time, it was allowed to reach room temperature, quenched by adding water (20 mL), and then extracted with EtOAc (50 mL).

The organic layer was washed with water (5 x 30 mL), dried over $MgSO_4$, filtered and the solvent was removed under reduced pressure. The crude was purified by silica gel chromatography (CH_2Cl_2/MeOH, 95:5) affording compound **19** as a white crystalline solid (0.58 g, 63%). ^{1}H NMR (300 MHz, $CDCl_3$): δ_H = 7.51 (s, 1H, H-2 Imidazole); 7.43 – 7.30 (m, 5H, Bn); 6.79 (s, 1H, H-4 Imidazole); 4.83 (s, 2H, OBn); 3.70 (t, *J* = 6.9 Hz, 2H, C$\underline{H}_2$-CH_2-imidazole); 2.90 (t, *J* = 6.9 Hz, 2H, CH_2-C$\underline{H}_2$-imidazole); 1.44 (s, 9H, ^{t}Bu). ^{13}C NMR (75 MHz, $CDCl_3$): δ_C = 155.4 (CO, Boc); 135.4 (C, C-5 Imidazole); 134.5 (CH, C-2 Imidazole); 129.4 (CH); 128.6 (CH); 128.4 (CH); 81.5 (C, ^{t}Bu); 76.9 (CH_2, OBn); 49.2 (CH_2, $\underline{C}H_2$-CH_2-imidazole); 28.2 (CH_3, ^{t}Bu); 24.4 (CH_2, CH_2-$\underline{C}H_2$-imidazole). HRMS (ESI+) calcd for $C_{17}H_{24}N_3O_3$ $[M+H]^+$ 318.1812, found 318.1831.

Compound 20.- A solution of **19** (0.40 g, 1.26 mmol) in a 1:5 TFA/CH_2Cl_2 mixture (12 mL) was stirred at room temperature for an hour. After this time, the solvent was removed under reduced pressure affording compound **20** as light yellow oil (0.55 g, 100%). ^{1}H NMR (300 MHz, CD_3OD): δ_H = 8.77 (d, *J* = 1.4 Hz, 1H, H-2 Imidazole); 7.57 – 7.02 (m, 6H); 5.01 (s, 2H, OBn); 3.59 (t, *J* = 7.1 Hz, 2H, C$\underline{H}_2$-CH_2-imidazole); 3.18 (t, *J* = 7.1 Hz, 2H, CH_2-C$\underline{H}_2$-imidazole). ^{13}C NMR (75 MHz, CD_3OD): δ_C = 134.2 (C, C-5 Imidazole); 133.6 (CH, C-2 Imidazole); 130.0 (C); 128.8 (CH); 128.7 (CH); 128.3 (CH); 116.7 (CH, C-4 Imidazole); 75.8 (CH_2, OBn); 48.5 (CH_2, $\underline{C}H_2$-CH_2-imidazole); 20.7 (CH_2, CH_2-$\underline{C}H_2$-imidazole). HRMS (ESI+) calcd for $C_{12}H_{16}N_3O$ $[M+H]^+$ 218.1287, found 218.1302.

Compound 21.- CDI (0.19 g, 1.21 mmol) was added to a cooled (0 ºC) solution of acid **16** in dry DMF. Then, it was allowed to reach the room temperature and stirred for an hour. After that time, it was cooled again to 0 ºC and a solution of benzyloxylamine **20** in DMF (5 mL) was added. The mixture was stirred at room temperature overnight. Then it was diluted with EtOAc (50 mL) and washed with water (30 mL) and brine (30 mL). The organic layer was dried over $MgSO_4$, filtered and solvent was removed under reduced pressure. The crude was purified by silica gel chromatography (CH_2Cl_2/MeOH, 8:2), affording compound **21** as a yellow amorphous solid (0.38 g, 69%). ^{1}H NMR (500 MHz, CD_3OD): δ_H = 8.75 (d, *J* = 1.4 Hz, 1H, H-15); 7.52 – 7.45 (m, 5H); 7.36 (d, *J* = 1.4 Hz, 1H, H-14); 7.25 – 7.22 (m, 2H, H-4/H-6); 7.09 (t, *J* = 8.0 Hz, 1H, H5); 5.68 (dc, *J* = 6.7, 2.5 Hz, 1H, H-9); 5.12 (d, *J* = 10.2 Hz, 1H, OBn); 5.00 (d, *J* = 10.2 Hz, 1H, OBn); 4.65 (hept, *J* = 6.1 Hz, 1H, –OC$\underline{H}$Me$_2$); 4.57 (hept, *J* = 6.0 Hz, 1H, –OC$\underline{H}$Me$_2$); 4.46 (d, *J* = 2.5 Hz, 1H, H-8); 4.36 (dt, *J* = 14.3, 6.8 Hz, 1H, H-11b); 3.90 (dt, *J* = 14.3, 6.8 Hz, 1H, H-11a); 3.17 – 3.00 (m, 2H, H-12); 1.42 (d, *J* = 6.7 Hz, 3H, Me); 1.35 (d, *J* = 6.1 Hz, 3H,

–OCH$\underline{Me_2}$); 1.34 (d, *J* = 6.1 Hz, 3H, –OCH$\underline{Me_2}$); 1.23 (d, *J* = 6.0 Hz, 3H, –OCH$\underline{Me_2}$); 1.22 (d, *J* = 6.0 Hz, 3H, –OCH$\underline{Me_2}$). ^{13}C NMR (125 MHz, CD_3OD): δ_C = 168.0 (CO, C-10); 166.4 (C, C-7); 152.9 (C, C-2); 148.5 (C, C-3); 135.1 (CH, C-15); 132.0 (C, C-13); 130.7 (CH); 130.6 (CH); 130.1 (CH); 127.4 (C, C-1); 124.7 (CH, C-6); 123.2 (CH, C-5); 120.4 (CH, C-4); 118.0 (CH, C-14); 78.0 (CH_2, OBn); 77.3 (CH, –O$\underline{C}$HMe$_2$); 72.2 (CH, –O$\underline{C}$HMe$_2$); 68.3 (CH, C-9); 55.9 (CH, C-8); 45.2 (CH_2, C-11); 23.0 (CH_2, C-12); 22.7 (CH_3, –OCH$\underline{Me_2}$); 22.3 (CH_3, –OCH$\underline{Me_2}$); 22.2 (CH_3, –OCH$\underline{Me_2}$); 22.1 (CH_3, –OCH$\underline{Me_2}$); 17.4 (CH_3, Me). HRMS (ESI+) calcd for $C_{29}H_{37}N_4O_5$ $[M+H]^+$ 521.2758, found 521.2742. $[\alpha]_D^{25}$ = +15.4 (c = 0.25, CH_3OH).

Compound 22.- A catalytic amount of Palladium over charcoal (5%) was added to a solution of compound **21** in MeOH and was stirred at room temperature in H_2 atmosphere (1 atm) for two hours. Afterwards, it was filtered through Celite and the solvent was removed under pressure affording compound **22** as a yellow amorphous solid (0.15 g, 95%). ^{1}H NMR (300 MHz, CD_3OD): δ = 8.70 (s, 1H, H-15); 7.34 (s, 1H, H-14); 7.25 (dd, *J* = 7.7, 1.6 Hz, 1H, H-6); 7.20 (dd, *J* = 8.3, 1.6 Hz, 1H, H-4); 7.08 (t, *J* = 7.9 Hz, 1H, H-5); 5.77 (cd, *J* = 6.7, 2.3 Hz, 1H, H-9); 4.69 (d, *J* = 2.3 Hz, 1H, H-8); 4.66-4.47 (m, 2H, m, –OC$\underline{H}$Me$_2$); 4.07 (dt, *J* = 13.6, 6.5 Hz, 1H, H-11b); 3.90 (dt, *J* = 13.7, 6.5 Hz, 1H, H-11a); 3.10 (t, *J* = 6.5 Hz, 2H, H-12); 1.50 (d, *J* = 6.7 Hz, 3H, Me); 1.37-1.19 (m, 12H, –OCH$\underline{Me_2}$). ^{13}C (75 MHz, CD_3OD): δ = 167.8 (CO, C9); 166.4 (C, C2'); 152.9 (C, C2"); 148.4 (C, C3"); 134.9 (CH, C-15); 132.2 (C, C-13); 127.8 (C, C-1); 124.7 (CH, C-6); 123.2 (CH, C-5); 120.4 (CH, C-4); 117.8 (CH, C-14); 77.4 (CH, –O$\underline{C}$HMe$_2$); 72.2 (CH, –O$\underline{C}$HMe$_2$); 68.7 (CH, C-9); 55.7 (CH, C-8); 48.2 (CH_2, C-11); 22.5 (CH_2, C-12); 22.4 (CH_3, –OCH$\underline{Me_2}$); 22.3 (CH_3, –OCH$\underline{Me_2}$); 22.0 (CH_3, –OCH$\underline{Me_2}$); 21.9 (CH_3, –OCH$\underline{Me_2}$); 17.1 (CH_3, Me). HRMS (ESI+) calcd for $C_{22}H_{31}N_4O_5$ $[M+H]^+$ 431.2288, found 431.2293. $[\alpha]_D^{23}$ = +19.4 (c = 0.25, CH_3OH).

Compound 23.- A solution of hydroxamate **22** (0.13 g, 0.30 mmol) in MeOH (20 mL) was stirred and refluxed for 1 hour. Then the solvent was removed under reduced pressure. The crude was purified by silica gel chromatography (CH_2Cl_2/MeOH, 9:1), to yield compound **23** as a light yellow oil (0.11 g, 87%). ^{1}H NMR (500 MHz, CD_3OD): δ_H = 7.66 (s, 1H, H-15); 7.42 (dd, *J* = 8.2, 1.7 Hz, 1H, H-6); 7.19 (dd, *J* = 8.2, 1.7 Hz, 1H, H-4); 7.13 (t, *J* = 8.2 Hz, 1H, H-5); 6.97 (s, 1H, H-14); 4.76 (hept, *J* = 6.2 Hz, 1H, –OC$\underline{H}$Me$_2$); 4.72 (d, *J* = 10.5 Hz, 1H, H-8); 4.66 (hept, *J* = 6.1 Hz, 1H, –OC$\underline{H}$Me$_2$); 4.42 (dc, *J* = 10.4, 6.1 Hz, 1H, H-9); 3.92 (dt, *J* = 13.9, 6.9 Hz, 1H, H-11b); 3.85 (dt, *J* = 14.0,

6.9 Hz, 1H, H-11a); 2.99 (t, *J* = 6.9 Hz, 2H, H-12); 1.53 (d, *J* = 6.2 Hz, 3H, Me); 1.36 (d, *J* = 6.2 Hz, 6H, –OCH$\underline{Me_2}$); 1.33 (d, *J* = 6.1 Hz, 3H, –OCH$\underline{Me_2}$); 1.29 (d, *J* = 6.1 Hz, 3H, –OCH$\underline{Me_2}$). ^{13}C NMR (125 MHz, CD_3OD): δ_C = 169.1 (CO, C-10); 168.4 (CO, C-7); 152.4 (C, C-2); 147.5 (C, C-3); 136.3 (CH, C-15); 129.6 (C, C-1); 124.9 (CH, C-6); 122.9 (CH, C-5); 120.3 (CH, C-4); 118.0 (CH, C-14); 81.1 (CH, C-9); 77.4 (CH, –O$\underline{C}$HMe$_2$); 72.5 (CH, –O$\underline{C}$HMe$_2$); 59.5 (CH, C-8); 46.0 (CH_2, C-11); 25.3 (CH_2, C-12); 22.6 (CH_3, –OCH$\underline{Me_2}$); 22.4 (CH_3, –OCH$\underline{Me_2}$); 22.3 (CH_3, –OCH$\underline{Me_2}$); 22.2 (CH_3, –OCH$\underline{Me_2}$); 17.5 (CH_3, Me). HRMS (ESI+) calcd for $C_{22}H_{31}N_4O_5$ $[M+H]^+$ 431.2288, found 431.2305. $[\alpha]_D^{26}$ = +25.9 (c = 0.52, CH_3OH).

Compound 1b·TFA.- Over a solution of compound **23** (50 mg, 0.12 mmol) in dry CH_2Cl_2 (12 mL) cooled to -78 ºC, was added dropwise a solution of BCl_3 in CH_2Cl_2 (1 M, 0.81 mL, 0.81 mmol). It was allowed to reach slowly -40 ºC and was stirred overnight. Then, water was added (5 mL) at -40 ºC, it was allowed to reach room temperature and was stirred for 20 minutes. Solvent was removed under reduced pressure and the crude was purified by HPLC using a Discovery® HS F5 (100 x 4.6 mm, 5 μm) column with a mobile phase consisting on a gradient 10% CH_3CN to 80% in H_2O (v/v), each containing 0.1% TFA, in 40 min at a flow rate of 1.0 mL/min (injected volume 0.2 mL; detection 254, 280, 320 nm), to afford compound **1b**·TFA as an amorphous beige solid (34 mg, 81%). ^{1}H NMR (500 MHz, CD_3OD): δ_H = 8.83 (s, 1H, H-15); 7.47 (s, 1H, H-14); 7.24 (dd, *J* = 8.1, 1.5 Hz, 1H, H-6); 6.96 (dd, *J* = 7.7, 1.0 Hz, 1H, H-4); 6.74 (t, *J* = 7.9 Hz, 1H, H-5); 4.63-4.51 (m, 2H, H-8/H-9); 4.02 (dt, *J* = 14.7, 6.5 Hz, 1H, H-11b); 3.90 (dt, *J* = 14.7, 6.2 Hz, 1H, H-11a); 3.13 (t, *J* = 6.5 Hz, 2H, H-12); 1.46 (d, *J* = 5.4 Hz, 3H, Me). ^{13}C NMR (125 MHz, CD_3OD): δ_C = 171.7 (CO, C-10); 169.1 (CO, C-7); 150.2 (C, C-2); 147.4 (C, C-3); 135.0 (CH, C-15); 132.0 (C, C-13); 120.2 (CH, C-4); 119.9 (CH, C-5); 119.0 (CH, C-6); 118.2 (CH, C-14); 116.3 (C, C-1); 79.7 (CH, C-9); 59.4 (CH, C-8); 44.9 (CH_2, C-11); 23.2 (CH_2, C-12); 17.2 (Me). HRMS (ESI+) calcd for $C_{16}H_{19}N_4O_5$ $[M+H]^+$ 347.1349, found 347.1361. $[\alpha]_D^{23}$ = +22.0 (c = 0.60, CH_3OH).

Synthesis of acinetobatin analogues 7-10

Compound 26.- A solution of D-cycloserine (**25**, 71 mg, 0.7 mmol) in water (0.33 mL) was treated with a solution of 2,3-bis(benzyloxy)benzoic acid (**24**, 250 mg, 0.7 mmol) in DMF (7 mL), PyBroP (426 mg, 0.91 mmol) and diisopropylethylamine (0.375 mL, 2.1 mmol). The resulting solution was stirred at room temperature for 12 h, and then transferred to separatory funnel. The organic layer was diluted with 5 mL ethyl acetate,

washed with 5 mL of an aqueous solution of hydrochloric acid (5%), followed by 5 mL of a saturated aqueous solution of sodium bicarbonate and 5 mL of water. The organic solution was then dried over magnesium sulfate, filtered and concentrated *in vacuo*. Purification by silica gel chromatography (hexane/EtOAc, 1:2) afforded amide **26** as an amorphous white solid (290 mg, 45%). ^{1}H NMR (300 MHz, $CDCl_3$): δ_H = 8.58 (d, *J* = 5.3 Hz, 1H, NH); 7.70 (dd, *J* = 7.4, 2.2 Hz, 1H, H-6); 7.52-7.24 (m, 10H); 7.22-7.10 (m, 2H); 5.25 (d, *J* = 10.6 Hz, 1H, OC$\underline{H}_2$-Ph); 5.17 (s, 2H, OC$\underline{H}_2$-Ph); 5.10 (d, *J* = 10.6 Hz, 1H, OC$\underline{H}_2$-Ph); 4.85 (ddd, *J* = 10.2, 8.1 Hz, 5.3, 1H, H-8); 4.77 (t, *J* = 8.1 Hz, 1H, H-9b); 3.81 (dd, *J* = 10.2, 8.1 Hz, 1H, H-9a). ^{13}C NMR (75 MHz, $CDCl_3$): δ_C = 165.9 (CO, C-7); 151.8 (C, C-2); 147.3 (C, C-3); 136.4 (C); 136.0 (C); 129.3 (CH); 128.7 (CH); 128.6 (CH); 128.5 (CH); 128.3 (CH); 127.7 (CH); 126.1 (C, C-1); 124.5 (CH, C-4); 123.4 (CH, C-5); 118.1 (CH, C-6); 76.7 (CH_2, O$\underline{C}H_2$-Ph); 74.7 (CH_2, C-9); 71.6 (CH_2, OC$\underline{H}_2$-Ph); 60.5 (CH, C-8). HRMS (ESI+) calcd for $C_{24}H_{23}N_2O_5$ $[M+H]^+$ 419.1598, found 419.1601. $[\alpha]_D^{25}$ = -8.6 (c = 0.41, $CHCl_3$).

Compound 27.- To a cooled solution (ice-bath) of 3-*Z*-aminopropanol (0.5 g, 2.85 mmol) and methanesulfonyl chloride (0.240 mL, 3.17 mmol) in dichloromethane (20 mL) was slowly added triethylamine (0.460 mL, 3.17 mmol). After stirring for 3 h at 0 ºC, the reaction mixture was concentrated and re-dissolved in ethyl acetate. The solution was washed with a 1M $KHSO_4$ aqueous solution, water (twice) and a saturated aqueous solution of sodium chloride, dried over magnesium sulfate and concentrated in vacuo. The mesylate **27** was obtained as a yellow solid (0.805 g, 93 %), which was directly used without further purification in the next step. ^{1}H NMR (300 MHz, $CDCl_3$): δ_H = 7.40-7.28 (m, 5H, Cbz); 5.09 (s, 2H, OC$\underline{H}_2$-Ph); 4.28 (t, *J* = 5.9 Hz, 2H, MsO-C$\underline{H}_2$-CH_2-CH_2-NHCbz); 3.33 (c, *J* = 6.3 Hz, 2H, MsO-CH_2-CH_2-C$\underline{H}_2$-NHCbz); 2.99 (s, 3H, SO_3-C$\underline{H}_3$); 1.95 (p, *J* = 6.2 Hz, 2H, MsO-CH_2-C$\underline{H}_2$-CH_2-NHCbz). ^{13}C NMR (75 MHz, $CDCl_3$): δ_C = 156.5 (CO, Cbz); 136.4 (C, Cbz); 128.5 (CH, Cbz); 128.2 (CH, Cbz); 128.0 (CH, Cbz); 127.5 (CH, Cbz); 127.3 (CH, Cbz); 67.2 (CH_2, Cbz); 66.8 (CH_2, MsO-$\underline{C}H_2$-CH_2-CH_2-NHCbz); 37.5 (CH_3, SO_3-$\underline{C}H_3$); 37.4 (CH_2, MsO-CH_2-CH_2-$\underline{C}H_2$-NHCbz); 29.5 (CH_2, MsO-CH_2-$\underline{C}H_2$-CH_2-NHCbz). HRMS (ESI+) calcd for $C_{12}H_{18}NO_5S$ $[M+H]^+$ 288.0861, found 288.0858.

Compound 28.- To a solution of amide **26** (83 mg, 0.2 mmol) in CH_3CN (9 mL) were added successively, mesylate **27** (104 mg, 0.36 mmol), sodium iodide (54 mg, 0.36 mmol) and sodium carbonate (100 mg, 0.72mmol). The suspension was stirred overnight at 60

ºC and then the solvent was removed under reduced pressure to give white solid residue. This crude material was purified by chromatography on silica gel column (hexane/EtOAc, 1:2 to 1:1) to give the expected amide **28** isolated as an amorphous white solid (76 mg, 56%). ^{1}H NMR (300 MHz, CD_3OD): δ_H = 8.55 (d, *J* = 5.5 Hz, 1H, NH); 7.67 (dd, *J* = 7.4, 2.2 Hz, 1H, H-6); 7.58-7.22 (m, 17H); 5.27-5.01 (m, 6H); 4.77 (ddd, *J* = 10.2, 8.3, 5.5 Hz, 1H, H-8); 4.64 (t, *J* = 8.3 Hz, 1H, H-9b); 3.77 (dd, *J* = 10.2, 8.3 Hz, 1H, H-9a); 3.70 – 3.52 (m, 2H, H-11); 3.22 (td, *J* = 6.3, 5.5 Hz, 2H, H-13); 1.78 (p, *J* = 6.3 Hz, 2H, H-12). ^{13}C NMR (75 MHz, CD_3OD): δ_C = 165.9 (CO, C-10); 165.6 (CO, C-7); 156.41 (CO, Cbz); 151.7 (C, C-2); 147.0 (C, C-3); 136.6 (C); 136.2 (C; 135.9 (C); 129.3 (CH); 128.7 (CH); 128.6 (CH); 128.5 (CH); 128.4 (CH); 128.3 (CH); 128.1 (CH); 128.0 (CH); 127.0 (CH); 126.0 (C, C-1); 124.4 (CH, C-4); 123.2 (CH, C-5); 117.8 (CH, C-6); 76.4 (CH_2, O<u>C</u>H_2-Ph); 72.4 (CH_2, C-9); 71.4 (CH_2, O<u>C</u>H_2-Ph); 66.5 (CH_2, Cbz); 52.6 (CH, C-8); 42.3 (CH_2, C-11); 37.7 (CH_2, C-13); 29.7 (CH_2, C-12). HRMS (ESI+) calcd for $C_{35}H_{36}N_3O_7$ $[M+H]^+$ 610.2547, found 610.2538. $[\alpha]_D^{24}$ = -11.6 (c = 0.12, $CHCl_3$).

Compound 7·TFA.- A suspension of amide **28** (50 mg, 0.08 mmol, 1 eq.) and 5% Pd/C (5 mg) in a mixture 4:1 MeOH:AcOH (2.5 mL) at room temperature was stirred under H_2 (1 atm) for 90 min. The reaction mixture was filtered through Celite and the solvent removed. The crude was subjected to purification by HPLC using a Discovery® XS F5 (100 x 4.6 mm, 5 µm) column with a mobile phase consisting on an isocratic 15% CH_3CN in H_2O (v/v), each containing 0.1% TFA, at a flow rate of 1.5 mL/min (injected volume 1 mL; detection 254 nm), to afford catechol **7**·TFA as an amorphous grayish solid (17 mg, 85%). ^{1}H NMR (500 MHz, CD_3OD): δ_H = 7.28 (dd, *J* = 8.1, 1.5 Hz, 1H, H-6); 6.98 (dd, *J* = 7.8, 1.5 Hz, 1H, H-4); 6.77 (t, *J* = 8.0, 1H, H-5); 5.04 (t, *J* = 9.5 Hz, 1H, H-9b); 4.69 (dd, , *J* = 9.5 Hz, *J* = 8.3 Hz, 1H, H-9a); 4.36 (dd, *J* = 9.5, 8.3 Hz, 1H, H-8); 3.86 (ddd, *J* = 15.0, 7.6, 5.9 Hz, 1H, H-11b); 3.69 (dt, *J* = 15.0, 5.9 Hz, 1H, H-11a); 3.10 (t, *J* = 12.5 Hz, 2H, H-13); 2.14-1.99 (m, 2H, H-12). ^{13}C NMR (125 MHz, CD_3OD): δ_C = 170.1 (CO, C-7); 166.8 (CO, C-10); 148.5 (C, C-2); 145.9 (C, C-3); 118.7 (CH, C-4); 118.5 (CH; C-5); 117.9 (CH, C-6); 115.1 (C, C-1); 70.1 (CH_2, C-9); 52.6 (CH, C-8); 42.0 (CH_2, C-11); 37.0 (CH_2, C-13); 24.8 (CH_2, C-12). HRMS (ESI+) calcd for $C_{13}H_{18}N_3O_5$ $[M+H]^+$ 296.1202, found 296.1194. $[\alpha]_D^{23}$ = -13.9 (c = 0.17, CH_3OH).

Compound 29.- To a solution of amide **26** (100 mg, 0.24 mmol) in CH_3CN (9 mL) were added successively, halides **18** (90 mg, 0.43 mmol) and sodium carbonate (100 mg, 0.72mmol). The suspension was stirred overnight at 60 ºC. The solvent was removed

under reduced pressure to give brownish oily residue. This crude material was purified by chromatography on silica gel column (dichloromethane/methanol, 95:5) to give the expected amide **29** isolated as a white crystalline solid (80 mg, 65%). ^{1}H NMR (300 MHz, $CDCl_3$: δ_H = 8.57 (d, *J* = 5.8 Hz, 1H, NH); 7.67 (dd, *J* = 7.4, 2.2 Hz, 1H, H-6); 7.54 – 7.10 (m, 13H); 6.81 (s, 1H, H-14); 5.22 (d, *J* = 10.6 Hz, 1H, OC$\underline{H}_2$-Ph); 5.16 (s, 2H, OC$\underline{H}_2$-Ph); 5.08 (d, *J* = 10.6 Hz, 1H, OC$\underline{H}_2$-Ph); 4.73 (ddd, *J* = 10.0, 8.5, 5.8 Hz, 1H, H-8); 4.60 (t, *J* = 8.4 Hz, 1H, H-9b); 3.98-3.72 (m, 3H, H-9a/H-11), 2.96 (t, *J* = 6.6 Hz, 2H, H-12). ^{13}C NMR (75 MHz, $CDCl_3$): δ_C = 165.7 (CO, C-10); 165.5 (CO, C-7); 151.6 (C, C-2); 146.9.5 (C, C-3); 136.2 (C, C-13); 136.0 (C); 135.2 (CH, C-14); 129.3 (CH); 128.7 (CH); 128.6 (CH); 128.5 (CH); 128.3 (CH); 127.7 (CH); 126.1 (C, C-1); 124.5 (CH, C-4); 123.1 (CH, C-5); 117.8 (CH, C-6); 76.5 (CH_2, O$\underline{C}H_2$-Ph); 71.8 (CH_2, C-9); 71.4 (CH_2, O$\underline{C}H_2$-Ph); 52.8 (CH, C-8); 45.1 (CH_2, C-11); 24.5 (CH_2, C-12). HRMS (ESI+) calcd for $C_{29}H_{29}N_4O_5$ $[M+H]^+$ 513.2132, found 513.2115. $[\alpha]_D^{25}$ = -20.1 (c = 1.17, CH_3OH).

Compound 8·TFA.- Compound **29** (30 mg, 0.06 mmol) was hydrogenated in a similar way as compound **12** to yield a crude which was subjected to purification by HPLC using a Discovery® HS F5 (100 x 4.6 mm, 5 μm) column with a mobile phase consisting on an isocratic 20% CH_3CN in H_2O (v/v), each containing 0.1% TFA, at a flow rate of 1.5 mL/min (injected volume 1 mL; detection 254 nm), to afford analogue **8**·TFA as an amorphous grayish solid (19 mg, 99%). ^{1}H NMR (500 MHz, CD_3OD): δ_H = 8.85 (s, 1H, H-15); 7.49 (s, 1H, H-14); 7.27 (dd, *J* = 8.2, 1.5 Hz, 1H, H-6); 6.98 (dd, *J* = 7.9, 1.5 Hz, 1H, H-4); 6.76 (t, *J* = 8.0 Hz, 1H, H-5); 4.99 (dd, *J* = 10.2, 9.0 Hz, 1H, H-9b); 4.67 (t, *J* = 8.7 Hz, 1H, H-9a); 4.29 (dd, *J* = 10.2, 8.3 Hz, 1H, H-8); 4.03 (dt, *J* = 14.8, 6.4 Hz, 1H, H-13b); 3.94 (dt, *J* = 14.8, 6.3 Hz, 1H, H-13a); 3.16 (t, *J* = 6.3 Hz, 2H, H-12). ^{13}C NMR (500 MHz, CD_3OD): δ_C = 170.0 (CO, C-10); 167.1 (CO, C-7); 148.5 (C, C-2); 145.9 (C, C-3); 133.6 (C, C-13); 130.6 (CH, C-15); 118.7 (CH, C-4); 118.5 (CH, C-5); 117.8 (CH, C-6); 116.8 (CH, C-14); 115.1 (C, C-1); 70.1 (CH_2, C-9); 52.4 (CH, C-8); 43.5 (CH_2, C-11); 21.7 (CH_2, C-12). HRMS (ESI+) calcd for $C_{15}H_{16}N_4O_5$ $[M+H]^+$ 333.1193, found 333.1198. $[\alpha]_D^{25}$ = -13.2 (c = 0.41, CH_3OH).

Compound 30.- To a cooled solution of 3-butyn-1-ol (0.53 g, 7.6 mmol) and methanesulfonyl chloride (0.64 mL, 8.3 mmol) in dichloromethane (7.5 mL) was slowly added triethylamine (1.21 mL, 8.3 mmol). After stirring for 3 h at 0 ºC, the reaction mixture was concentrated and re-dissolved in ethyl acetate. The solution was washed with 1M $KHSO_4$ aqueous solution, water (twice) and a saturated aqueous solution of sodium

chloride, dried over magnesium sulfate and concentrated in vacuo. The mesylate **30** was obtained as a yellow solid (1.12 g, 99%), which was directly used without further purification in the next step. ^{1}H NMR (300 MHz, $CDCl_3$): δ_H = 4.26 (t, *J* = 6.7, 2H, H-4); 3.02 (s, 3H, OMs); 2.66-2.58 (m, 2H, H-3); 2.05 (t, *J* = 2.7 Hz, 1H, H-1).^{13}C NMR (75 MHz, $CDCl_3$): δ_C = 79.1 (CH, C-1); 71.5 (C, C-2); 67.6 (CH_2, C-4); 38.3 (CH_3, OMs); 20.3 (CH_2, C-3). HRMS (ESI+) calcd for $C_5H_9O_3S$ $[M+H]^+$ 149.0266, found 149.0271.

Compound 31.- To a solution of amide **26** (150 mg, 0.34 mmol), NaI (51 mg, 0.34 mmol) and Na_2CO_3 (85 mg, 0.58 mmol) in CH_3CN (12 mL) was added mesylate **30** (86 mg, 0.58 mmol) and the mixture was stirred at 60 ºC overnight. After cooling to room temperature, the reaction mixture was concentrated under reduced pressure. The residue was purified by silica gel column chromatography (hexane/EtOAc, 2:1) to afford alkyne **31** as a white crystalline solid (93 mg, 61%). ^{1}H NMR (300 MHz, $CDCl_3$): δ_H = 8.56 (d, *J* = 5.4 Hz, 1H, NH); 7.68 (dd, *J* = 7.4, 2.2 Hz, 1H, H-6); 7.52-7.23 (m, 10H); 7.23 – 7.09 (m, 2H);); 5.26 (d, *J* = 10.6 Hz, 1H, O-C$\underline{H}_2$-Ph); 5.19 (s, 2H, O-C$\underline{H}_2$-Ph); 5.11 (d, *J* = 10.7 Hz, 1H, O-C$\underline{H}_2$-Ph)); 4.87 (ddd, *J* = 10.3, 8.3, 5.1, 1H, H-8); 4.71 (t, *J* = 8.3 Hz, 1H, H-9b); 3.83 – 3.68 (m, 3H, H-9a/H-13); 2.53 (tdd, *J* = 7.0, 2.7, 1.1 Hz, 2H, H-12); 1.98 (t, *J* = 2.6 Hz, 1H, H-14). ^{13}C NMR (75 MHz, $CDCl_3$): δ_C = 166.5 (CO, C-10); 165.6 (CO, C-7); 151.1 (C, C-2); 147.0 (C, C-3); 136.2 (C); 135.9 (C); 129.3 (CH); 128.7 (CH); 128.6 (CH); 128.5 (CH); 128.3 (CH); 127.7 (CH); 126.1 (C, C-1); 124.4 (CH, C-4); 123.2 (CH, C-5); 117.8 (CH, C-6); 80.0 (CH, C-14); 76.4 (CH_2, O-C$\underline{H}_2$-Ph); 72.7 (CH_2, C-9); 71.4 (CH_2, O-C$\underline{H}_2$-Ph); 70.5 (C, C-13); 52.5 (CH, C-8); 43.8 (CH_2, C-11); 17.1 (CH_2, C-12). HRMS (ESI+) calcd for $C_{28}H_{27}N_2O_5$ $[M+H]^+$ 471.1914, found 471.1911. $[\alpha]_D^{25}$ = -18.3 (c = 0.30, $CHCl_3$).

Compound 32.- Trimethylsilyl azide (0.032 mL, 0.24 mmol) was added to a DMF and MeOH solution (2 mL, 9:1) of CuI (2.1 mg, 0.008 mmol) and alkyne **31** (77 mg, 0.16 mmol) under Ar in a 10 mL round bottomed flask. The reaction mixture was stirred at 100 ºC for 12 h. After consumption of alkyne **31**, the mixture was cooled to room temperature, diluted with ethyl acetate (10 mL) and washed with a saturated aqueous solution of sodium chloride (10 mL). The organic phase was conserved and the aqueous phase was extracted with ethyl acetate (3 x 10 mL). All the organic phases were dried over magnesium sulfate, filtered and concentrated *in vacuo*. The residue was purified by silica gel column chromatography (dichloromethane/methanol: 98:2 to 95:5) to afford the 1,2,3-triazole **32** as an amorphous grayish solid (70 mg, 86%). ^{1}H NMR (300 MHz,

CD_3OD): δ_H = 7.71 (s, 1H, H-14); 7.51 (dd, *J* = 8.1, 1.4 Hz, 1H, H-6); 7.45 – 7.23 (m, 11H), 7.16 (t, *J* = 8.0 Hz, 1H, H-5); 5.22-5.04 (m, 4H); 4.57 (t, *J* = 8.5 Hz, 1H, H-9b); 3.93-3.86 (m, 3H, H-9a/H-11), 3.10 (td, *J* = 6.8, 3.1 Hz, 2H, H-12). ^{13}C NMR (75 MHz, CD_3OD): δ_C = 166.9 (CO, C-10); 166.4 (CO, C-7); 152.0 (C, C-2); 146.1(C, C-3); 136.7 (C); 136.5 (C); 128.8 (CH); 128.3 (CH); 128.2 (CH); 128.1 (CH); 127.8 (CH); 127.7 (CH); 127.2 (C, C-1); 124.1 (CH, C-4); 121.5 (CH, C-5); 117.4 (CH, C-6); 76.6 (CH_2, O-$\underline{C}H_2$-Ph); 70.9 (CH_2, C-9); 70.8 (CH_2, O-$\underline{C}H_2$-Ph); 52.5 (CH, C-8); 44.4 (CH_2, C-11); 22.0 (CH_2, C-12). HRMS (ESI+) calcd for $C_{28}H_{28}N_5O_5$ $[M+H]^+$ 514.2084, found 514.2064. $[\alpha]_D^{25}$ = -10.7 (c = 0.99, CH_3OH).

Compound 9·TFA.- Compound **32** (25 mg, 0.05 mmol) was hydrogenated in a similar way as compound **28** to yield a crude which was subjected to purification by HPLC using a Discovery® XS F5 (100 x 4.6 mm, 5 μm) column with a mobile phase consisting on an isocratic 10% CH_3CN in H_2O (v/v), each containing 0.1% TFA, at a flow rate of 1.5 mL/min (injected volume 1 mL; detection 254 nm), to afford 2,3-dihidroxibenzamida **9**·TFA as an amorphous grayish solid (9 mg, 72%). ^{1}H NMR (500 MHz, CD_3OD): δ_H = 7.80 (s, 1H, H-14); 7.28 (dd, *J* = 8.2, 1.5 Hz, 1H, H-6); 6.97 (dd, *J* = 7.9, 1.4 Hz, 1H, H-4); 6.75 (t, *J* = 8.0 Hz, 1H, H-5); 5.08 (dd, *J* = 10.2, 8.7 Hz, 1H, H-9b); 4.69 (td, *J* = 8.6, 1.4 Hz, 1H, H-9a); 4.23 (ddd, *J* = 9.9, 8.4, 1.2 Hz, 1H, H-8); 4.04-3.86 (m, 2H, H-11), 3.16 (t, *J* = 6.7 Hz, 2H, H-12). ^{13}C NMR (125 MHz, CD_3OD): δ_C = 170.2 (CO, C-10); 166.8 (CO, C-7); 148.5 (C, C-2); 146.0 (C, C-3); 142.0 (C, C-13); 128.2 (CH, C-14); 118.7 (CH, C-4); 118.4 (CH, C-5); 117.7 (CH, C-6); 114.9 (C, C-1); 70.5 (CH_2, C-9); 52.3 (CH, C-8); 44.5 (CH_2, C-11); 22.5 (CH_2, C-12). HRMS (ESI+) calcd for $C_{14}H_{16}N_5O_5$ $[M+H]^+$ 334.1145, found 334.1141. $[\alpha]_D^{25}$ = -8.2 (c = 0.37, CH_3OH).

Compound 33.- To a stirred solution of mesylate **30** (105 mg, 0.37 mmol) in anhydrous DMF was added sodium azide (55 mg, 0.55 mmol in one portion at room temperature. The mixture was stirred at 80 ºC for 3 h. The reaction mixture was allowed to cool to room temperature, water was added and then it was extracted with EtOAc (3 x 10 mL). The combined organic layers were washed with a saturated aqueous solution of sodium chloride and dried over anhydrous magnesium sulfate and filtered. After concentration under reduced pressure, a brownish oily residue was obtained. This crude material was purified by chromatography on silica gel column (hexane/EtOAc, 1:3) to give the expected azide **33** isolated as a dark brown liquid (65 mg, 81%). ^{1}H NMR (300 MHz, $CDCl_3$): δ_H = 7.43 – 7.26 (m, 5H, Cbz); 5.11 (s, 2H, O-C$\underline{H}_2$-Ph); 3.36 (t, *J* = 6.6 Hz, 2H,

CH_2-C<u>H_2</u>-N_3); 3.31 – 3.22 (m, 2H, CbzNH-C<u>H_2</u>), 1.79 (p, *J* = 6.6 Hz, 2H, C<u>H_2</u>-CH_2-N_3). ^{13}C NMR (75 MHz, $CDCl_3$): δ_C =156.4 (CO, Cbz); 136.4 (C, Cbz); 128.5 (CH, Cbz); 128.2 (CH, Cbz); 128.1 (CH, Cbz); 127.8 (CH, Cbz); 127.5 (CH, Cbz); 66.8 (CH_2, Cbz); 49.0 (CH_2, CbzNH-<u>C</u>H_2); 38.5 (CH_2, CH_2-<u>C</u>H_2-N_3); 29.1 (CH_2, <u>C</u>H_2-CH_2-N_3). HRMS (ESI+) calcd for $C_{11}H_{15}N_4O_2$ $[M+H]^+$ 235.1189, found 235.1193.

Compound 34. To a stirred solution of alkyne **31** (100 mg, 0.22 mmol) in anhydrous THF (2 mL) were added successively a solution of azide **33** (40 mg, 0.18 mmol) in anhydrous THF (2 mL), CuI (4 mg, 0.1 eq) and diisopropylethylamine (0.04 mL, 0.09 mmol). The solution was stirred for 12 h at room temperature. After that time, the reaction was quenched with water, transferred to a separatory funnel and diluted with 5 mL of ethyl acetate. The organic layer was washed with 5 mL of a saturated aqueous solution of sodium chloride, dried over magnesium sulfate, filtered and concentrated *in vacuo*. Purification by silica gel chromatography (CH_2Cl_2/MeOH, 99:1) afforded triazole **34** as an amorphous grayish solid (125 mg, 99%). ^{1}H NMR (300 MHz, $CDCl_3$): δ_H = 8.47 (d, *J* = 5.8 Hz, 1H, NH); 7.64 (dd, *J* = 7.6, 2.0 Hz, 1H, H-6); 7.51 (s, 1H, H-14); 7.49-7.21 (m, 15H); 7.18 – 7.06 (m, 2H); 5.27-5.01 (m, 6H); 4.74 (ddd, *J* = 10.3, 8.4, 5.8 Hz, 1H, H-8); 4.60 (t, *J* = 8.3 Hz, 1H, H-9b); 4.32 (t, *J* = 6.6 Hz, 2H, H-15); 3.87 (p, *J* = 7.1 Hz, 2H, H-11); 3.77 (dd, *J* = 10.4, 8.3 Hz, 1H, H-9a); 3.10 (m, 4H, H-17/H-12); 2.05 (dd, *J* = 7.1 Hz, 2H, H-16). ^{13}C NMR (75 MHz, $CDCl_3$): δ_C = 166.0 (CO, C-10); 165.4 (CO, C-7); 151.7 (CO, Cbz); 146.8 (C, C-2); 137.8 (C, C-3); 136.5 (C); 136.2 (C); 134.5 (C); 129.4 (CH); 128.7 (CH); 128.6 (CH); 128.5 (CH); 128.4 (CH); 218.3 (CH); 128.1 (CH); 128.0 (CH); 127.7 (CH); 126.1 (C, C-1); 124.5 (CH, C-4); 123.1 (CH, C-5); 117.5 (CH, C-6); 76.4 (CH_2, O-<u>C</u>H_2-Ph); 71.9 (CH_2, C-9); 71.4 (CH_2, O-<u>C</u>H_2-Ph); 66.7 (CH_2, Cbz); 52.6 (CH, C-8); 47.2 (CH_2, C-11); 44.5 (CH_2, C-15); 37.5 (CH_2, C-17); 30.5 (CH_2, C-16); 23.4 (CH_2, C-12). HRMS (ESI+) calcd for $C_{39}H_{41}N_6O_7$ $[M+H]^+$ 705.3031, found 705.3012. $[\alpha]_D^{25}$ = -5.2 (c = 0.80, $CHCl_3$).

Compound 10·TFA.- Compound **34** (40 mg, 0.06 mmol) was hydrogenated in a similar way as compound **28** to yield a crude which was subjected to purification by HPLC using a Discovery® HS F5 (100 x 4.6 mm, 5 μm) column with a mobile phase consisting on an isocratic 20% CH_3CN in H_2O (v/v), each containing 0.1% TFA, at a flow rate of 1.5 mL/min (injected volume 1 mL; detection 254 nm), to give the expected analogue **10**·TFA isolated as an amorphous grayish solid (15 mg, 72%). ^{1}H NMR (500 MHz, D_2O): δ_H = 7.83 (s, 1H, H-14); 7.15 (dd, *J* = 8.1, 1.5 Hz, 1H, H-6); 7.01 (dd, *J* = 7.9, 1.5 Hz, 1H,

H-4); 6.78 (t, *J* = 8.0 Hz, 1H, H-5); 4.95 (t, *J* = 9.4 Hz, 1H, H-9b); 4.60 (t, *J* = 8.9 Hz, 1H, H-9a); 4.44 (t, *J* = 6.8 Hz, 2H, H-15); 4.25 (dd, *J* = 9.4, 8.9 Hz, 1H, H8); 3.94 - 4.07 (m, 2H, H11); 3.06 (t, *J* = 6.2 Hz, 2H, H-17); 2.87 (t, *J* = 7.5 Hz, 2H, H-12); 2.18 (p, *J* = 6.5 Hz, 2H, H-16). ^{13}C NMR (125 MHz, D_2O): δ_C = 170.1 (CO, C-10); 166.4 (CO, C-7); 164.8 (C, C-13); 147.1 (C, C-2); 144.6 (C, C-3); 124.4 (CH, C-14); 119.9 (CH, C-4); 119.8 (CH, C-5); 119.2 (CH, C-6); 116.1 (C, C-1); 70.0 (CH_2, C-9); 52.7 (CH, C-8); 47.5 (CH_2, C-11); 44.8 (CH_2, C-15); 36.5 (CH_2, C-17); 27.1 (CH_2, C-16); 21.8 (CH_2, C-12). HRMS (ESI+) calcd for $C_{17}H_{23}N_6O_5$ $[M+H]^+$ 391.1724, found 391.1718. $[\alpha]_D^{25}$ = -12.3 (c = 0.24, CH_3OH).

Compound 35.- Trimethylsilyl azide (0.13 mL, 1.01 mmol) was added to a DMF and MeOH solution (2 mL, 9:1) of CuI (7 mg, 0.03 mmol) and alkyne **30** (100 mg, 0.68 mmol) under Ar in a 10 mL round bottomed flask. The reaction mixture was stirred at 100 ºC for 12 h. After consumption of alkyne **30**, the mixture was cooled to room temperature, diluted with ethyl acetate (10 mL) and washed with a saturated aqueous solution of sodium chloride (10 mL). The organic phase was conserved and the aqueous phase was extracted with ethyl acetate (2 x 10 mL). All the organic phases were dried over magnesium sulfate, filtered and concentrated *in vacuo* to afford the 1,2,3-triazole **35** as an amorphous grayish solid (130 mg, quant.). ^{1}H NMR (300 MHz, $CDCl_3$): δ_H = 7.55 (s, 1H, H-4 triazole); 4.34 - 4.54 (m, 4.42, 2H, H-1); 3.19 (t, *J* = 6.6 Hz, 1H, H-2b); 3.11 (t, *J* = 6.6 Hz, H-2a); 2.96 (s, 3H, OMs). LRMS (ESI+) = 192.04 $[M+H]^+$.

Compound 32 from 35.- To a solution of amide **26** (120 mg, 0.28 mmol) in CH_3CN (10 mL) were added successively mesylate **35** (92 mg, 0.48 mmol), sodium iodide (41 mg, 0.28 mmol) and sodium carbonate (70 mg, 0.48 mmol). The suspension was stirred overnight at 60 ºC and then the solvent was removed under reduced pressure to give white solid residue. This crude material was purified by chromatography on silica gel column (CH_2Cl_2/MeOH, 99:1) to give the expected amide **32** isolated as a white crystalline solid (80 mg, 52%).

Compound 36.- To a stirred solution of alkyne **30** (41 mg, 0.27 mmol) in anhydrous THF (3 mL) were added successively a solution of azide **33** (50 mg, 0.23 mmol) in anhydrous THF (2 mL), CuI (5 mg, 0.02 mmol) and diisopropylethylamine (0.05 mL, 0.11 mmol). The solution was stirred for 12 h at room temperature. After that time, the reaction was quenched with water, transferred to a separatory funnel and diluted with 5 mL of ethyl acetate. The organic layer was washed with 5 mL of a saturated aqueous solution of

sodium chloride, dried over magnesium sulfate, filtered and concentrated *in vacuo* to afford triazole **36** as an amorphous yellow solid (102 mg, 99%). ^{1}H NMR (300 MHz, $CDCl_3$): δ_H = 7.57 (s, 1H, H-4 triazole); 7.34 (s, 5H, Cbz); 5.08 (s, 2H, Cbz); 4.42 (t, *J* = 6.2 Hz, 2H, H-1); 4.33 (t, *J* = 6.7 Hz, 2H, H-5); 3.25 - 3.15 (m, 4H, H-2/H-7); 2.88 (s, 3H); 2.06 - 1.97 (m, 2H, H-6). ^{13}C NMR (75 MHz, $CDCl_3$): δ_C = 156.7 (CO, Cbz); 136.5 (C); 128.7 (CH); 128.3 (CH); 128.2 (CH); 68.8 (CH_2, Cbz); 66.9 (CH_2, C-1); 47.7 (CH_2, C-5); 37.8 (CH_2, C-7); 37.5 (CH_3, OMs); 30.6 (CH_2, C-6); 26.2 (CH_2, C-2). HRMS (ESI+) calcd. for $C_{16}H_{23}N_4O_5S$ $[M+H]^+$ 383.1383, found 383.1385.

Compound 34 from 36.- To a solution of amide **26** (76 mg, 0.18 mmol) in CH_3CN (4 mL) were added successively mesylate **36** (70 mg, 0.18 mmol), sodium iodide (30 mg, 0.18 mmol) and sodium carbonate (46 mg, 0.31 mmol). The suspension was stirred overnight at 60 ºC and then the solvent was removed under reduced pressure to give white solid residue. This crude material was purified by chromatography on silica gel column (hexane/EtOAc, 1:3) to give the expected amide **34** isolated as an amorphous grayish solid (77 mg, 61%).

ASSOCIATED CONTENT

Supporting Information

The Supporting Information is available free of charge on the ACS Publications website.

Figure S1. Pictures of cross-feeding assays; Figure S2. Alignment of *fstA* (GI:1143382) and *fstB* (GI:41745840); Figure S3. Alignment of FstA (GI:1143382) and FstB (GI:41745840) amino acids sequences; Figure S4. Growth curves of *A. salmonicida fstB*(+) and *fstB*(-) strains with the addition of Acb (**1a**), *ent*-Acb (**1b**), or analogues **7**-**10**; Table S1. Strains and plasmids used in this study; Table S2. Primers used for mutant construction, genetic complementation and strain screening by PCR; NMR spectra of compounds **1b**, **7**-**10**, **12**-**36**; Comparison between spectra of acinetobactin and *ent*-acinetobactin; HPLC chromatograms of crude reactions.

AUTHOR INFORMATION

Corresponding Authors

*Manuel L. Lemos, E-mail manuel.lemos@usc.es. Phone: +34-881816080

*Jaime Rodríguez, E-mail: jaime.rodriguez@udc.es. Phone: +34-981167000

*Carlos Jiménez, E-mail: carlos.jimenez@udc.es. Phone: +34-981167000

Notes

The authors declare no competing financial interest.

ACKNOWLEDGMENTS

This work was supported by grant AGL2015-63740-C2-1/2-R from Spanish Ministry of Economy and Competitiveness (MINECO), and by grant 10PXIB235157PR from Xunta de Galicia, Spain; both co-funded by the FEDER Programme from the European Union.

REFERENCES

(1) Ratledge, C., and Dover, L. G. (2000) Iron Metabolism in Pathogenic Bacteria. *Annu. Rev. Microbiol. 54*, 881–941.
(2) Wandersman, C., and Delepelaire, P. (2004) Bacterial Iron Sources: From Siderophores to Hemophores. *Annu. Rev. Microbiol. 58*, 611–647.
(3) Ganz, T., and Nemeth, E. (2015) Iron homeostasis in host defence and inflammation. *Nat. Rev. Immunol. 15*, 500–510.
(4) Miethke, M., and Marahiel, M. A. (2007) Siderophore-Based Iron Acquisition and Pathogen Control. *Microbiol. Mol. Biol. Rev. 71*, 413–451.
(5) Cordero, O. X., Ventouras, L.-A., DeLong, E. F., and Polz, M. F. (2012) Public good dynamics drive evolution of iron acquisition strategies in natural bacterioplankton populations. *Proc. Natl. Acad. Sci. 109*, 20059–20064.
(6) Toranzo, A. E., Magariños, B., and Romalde, J. L. (2005) A review of the main bacterial fish diseases in mariculture systems. *Aquaculture 246*, 37–61.
(7) Balado, M., Souto, A., Vences, A., Careaga, V. P., Valderrama, K., Segade, Y., Rodríguez, J., Osorio, C. R., Jiménez, C., and Lemos, M. L. (2015) Two catechol siderophores, acinetobactin and amonabactin, are simultaneously produced by Aeromonas salmonicida subsp. salmonicida sharing part of the biosynthetic pathway. *ACS Chem. Biol. 10*, 2850–2860.
(8) Yamamoto, S., Sakakibara, Y., and Okujo, N. (1994) Isolation and structure elucidation of acinetobactin, a novel siderophore from Acinetobacter baumannii. *Arch. Microbiol. 162*, 249–254.
(9) Telford, J. R., Leary, J. A., Tunstad, L. M. G., Byers, B. R., and Raymond, K. N. (1994) Amonabactin: Characterization of a series of siderophores from Aeromonas hydrophila. *J. Am. Chem. Soc. 116*, 4499–4500.
(10) Matthijs, S., Laus, G., Meyer, J.-M., Abbaspour-Tehrani, K., Schäfer, M., Budzikiewicz, H., and Cornelis, P. (2009) Siderophore-mediated iron acquisition in the entomopathogenic bacterium Pseudomonas entomophila L48 and its close relative Pseudomonas putida KT2440. *Biometals 22*, 951–964.
(11) Mihara, K. (2004) Identification and transcriptional organization of a gene cluster involved in biosynthesis and transport of acinetobactin, a siderophore produced by Acinetobacter baumannii ATCC 19606T. *Microbiology 150*, 2587–2597.
(12) Ebanks, R. O., Dacanay, A., Goguen, M., Pinto, D. M., and Ross, N. W. (2004) Differential proteomic analysis of Aeromonas salmonicida outer membrane proteins in response to low iron andin vivo growth conditions. *Proteomics 4*, 1074–1085.
(13) Rattanachaikunsopon, P., and Phumkhachorn, P. (2012) Detection of Aeromonas salmonicida by Reverse Transcription-Multiplex Polymerase Chain Reaction. *Biosci. Biotechnol. Biochem. 76*, 665–670.
(14) Beaz-Hidalgo, R., Magi, G. E., Balboa, S., Barja, J. L., and Romalde, J. L. (2008) Development of a PCR protocol for the detection of Aeromonas salmonicida in fish by amplification of the fstA (ferric siderophore receptor) gene. *Vet. Microbiol. 128*, 386–394.
(15) Möllmann, U., Heinisch, L., Bauernfeind, A., Köhler, T., and Ankel-Fuchs, D. (2009) Siderophores as drug delivery agents: application of the “Trojan Horse” strategy. *Biometals 22*, 615–624.
(16) Carvalho, C. C. C. R. de, and Fernandes, P. (2014) Siderophores as “Trojan Horses”: tackling multidrug resistance? *Front. Microbiol. 5*, 290–293.
(17) Reith, M. E., Singh, R. K., Curtis, B., Boyd, J. M., Bouevitch, A., Kimball, J.,

Munholland, J., Murphy, C., Sarty, D., Williams, J., Nash, J. H., Johnson, S. C., and Brown, L. L. (2008) The genome of Aeromonas salmonicida subsp. salmonicida A449: insights into the evolution of a fish pathogen. *BMC Genomic- 9*, 427.
(18) Najimi, M., Lemos, M. L., and Osorio, C. R. (2008) Identification of siderophore biosynthesis genes essential for growth of Aeromonas salmonicida under iron limitation conditions. *Appl. Environ. Microbiol. 74*, 2341–2348.
(19) Schwyn, B., and Neilands, J. B. (1987) Universal chemical assay for the detection and determination of siderophores. *Anal. Biochem. 160*, 47–56.
(20) Noinaj, N., Guillier, M., Barnard, T. J., and Buchanan, S. K. (2010) TonB-dependent transporters: regulation, structure, and function. *Annu. Rev. Microbiol. 64*, 43–60.
(21) Wuest, W. M., Sattely, E. S., and Walsh, C. T. (2009) Three siderophores from one bacterial enzymatic assembly line. *J. Am. Chem. Soc. 131*, 5056–5057.
(22) Shapiro, J. A., and Wencewicz, T. A. (2016) Acinetobactin isomerization enables adaptive iron acquisition in *Acinetobacter baumannii* through pH-triggered siderophore swapping. *ACS Infect. Dis. 2*, 157–168.
(23) Sattely, E. S., and Walsh, C. T. (2008) A latent oxazoline electrophile for N−O−C bond formation in pseudomonine biosynthesis. *J. Am. Chem. Soc. 130*, 12282–12284.
(24) Anthoni, U., Christophersen, C., Nielsen, P. H., Gram, L., and Petersen, B. O. (1995) Pseudomonine, an isoxazolidone with siderophoric activity from Pseudomonas fluorescens AH2 isolated from lake Victorian Nile Perch. *J. Nat. Prod. 58*, 1786–1789.
(25) Takeuchi, Y., Ozaki, S., Satoh, M., Mimura, K., Hara, S., Abe, H., Nishioka, H., and Harayama, T. (2010) Synthesis of Acinetobactin. *Chem. Pharm. Bull. 58*, 1552–1553.
(26) Souto, A., Montaos, M. A., Balado, M., Osorio, C. R., Rodríguez, J., Lemos, M. L., and Jiménez, C. (2013) Synthesis and antibacterial activity of conjugates between norfloxacin and analogues of the siderophore vanchrobactin. *Bioorg. Med. Chem. 21*, 295–302.
(27) Hanessian, S., Vakiti, R. R., Dorich, S., Banerjee, S., Lecomte, F., DelValle, J. R., Zhang, J., and Deschênes-Simard, B. (2011) Total synthesis of pactamycin. *Angew. Chem. Int. Ed. 50*, 3497–3500.
(28) Fennell, K. A., and Miller, M. J. (2007) Syntheses of amamistatin fragments and determination of their HDAC and antitumor Activity. *Org. Lett. 9*, 1683–1685.
(29) Soengas, R. G., Anta, C., Espada, A., Nieto, R. M., Larrosa, M., Rodríguez, J., and Jiménez, C. (2007) Vanchrobactin: absolute configuration and total synthesis. *Tetrahedron Lett. 48*, 3021–3024.
(30) Moorhouse, A. D., and Moses, J. E. (2008) Click chemistry and medicinal chemistry: A Case of "Cyclo-Addiction." *Chem. Med. Chem. 3*, 715–723.
(31) Jin, T., Kamijo, S., and Yamamoto, Y. (2004) Copper-catalyzed synthesis of N-unsubstituted 1,2,3-triazoles from nonactivated terminal alkynes. *Eur. J. Org. Chem. 2004*, 3789–3791.
(32) Tornøe, C. W., Christensen, C., and Meldal, M. (2002) Peptidotriazoles on solid phase: [1,2,3]-triazoles by regiospecific copper(I)-catalyzed 1,3-dipolar cycloadditions of terminal alkynes to azides. *J. Org. Chem. 67*, 3057–3064.
(33) Soengas, R. G., Larrosa, M., Balado, M., Rodriguez, J., Lemos, M. L., and Jimenez, C. (2008) Synthesis and biological activity of analogues of vanchrobactin, a siderophore from Vibrio anguillarum serotype O2. *Org. Biomol. Chem. 6*, 1278–1287.
(34) Soengas, R. G., Anta, C., Espada, A., Paz, V., Ares, I. R., Balado, M., Rodríguez, J., Lemos, M. L., and Jiménez, C. (2006) Structural characterization of vanchrobactin, a new catechol siderophore produced by the fish pathogen Vibrio anguillarum serotype O2. *Tetrahedron Lett. 47*, 7113–7116.
(35) Abergel, R. J., Zawadzka, A. M., Hoette, T. M., and Raymond, K. N. (2009)

Enzymatic hydrolysis of trilactone siderophores: where chiral recognition occurs in enterobactin and bacillibactin iron transport. *J. Am. Chem. Soc. 131*, 12682–12692.
(36) Youard, Z. A., Wenner, N., and Reimmann, C. (2010) Iron acquisition with the natural siderophore enantiomers pyochelin and enantio-pyochelin in Pseudomonas species. *BioMetals 24*, 513–522.
(37) Carvalho, C. C. C. R. de, and Fernandes, M. P. C. M. and P. (2011) Recent achievements on siderophore production and application. *Recent Patents Biotechnol. 5*, 183–198.
(38) Noël, S., Guillon, L., Schalk, I. J., and Mislin, G. L. A. (2011) Synthesis of fluorescent probes based on the pyochelin siderophore scaffold. *Org. Lett. 13*, 844–847.
(39) Abergel, R. J., and Raymond, K. N. (2011) Multidentate terephthalamidate and hydroxypyridonate ligands: towards new orally active chelators. *Hemoglobin 35*, 276–290.
(40) Mislin, G. L. A., and Schalk, I. J. (2014) Siderophore-dependent iron uptake systems as gates for antibiotic Trojan horse strategies against Pseudomonas aeruginosa. *Metallomics 6*, 408–420.
(41) Bergeron, R. J., Bharti, N., Singh, S., McManis, J. S., Wiegand, J., and Green, L. G. (2009) Vibriobactin antibodies: a vaccine strategy. *J. Med. Chem. 52*, 3801–3813.
(42) Zhou, H., Zhang, T., Yu, D., Pi, B., Yang, Q., Zhou, J., Hu, S., and Yu, Y. (2011) Genomic analysis of the multidrug-resistant Acinetobacter baumannii strain MDR-ZJ06 widely spread in China. *Antimicrob. Agents Chemother. 55*, 4506–4512.
(43) Miller, J. H. (1972) Experiments in molecular genetics. Cold Spring Harbor Laboratory Press, Cold Spring Harbor, NY.
(44) Altschul, S. F., Gish, W., Miller, W., Myers, E. W., and Lipman, D. J. (1990) Basic local alignment search tool. *J. Mol. Biol. 215*, 403–410.
(45) Petersen, T. N., Brunak, S., von Heijne, G., and Nielsen, H. (2011) SignalP 4.0: discriminating signal peptides from transmembrane regions. *Nat. Meth. 8*, 785–786.
(46) Finn, R. D., Bateman, A., Clements, J., Coggill, P., Eberhardt, R. Y., Eddy, S. R., Heger, A., Hetherington, K., Holm, L., Mistry, J., Sonnhammer, E. L. L., Tate, J., and Punta, M. (2014) Pfam: the protein families database. *Nucleic Acids Res. 42*, 222–230.
(47) Biasini, M., Bienert, S., Waterhouse, A., Arnold, K., Studer, G., Schmidt, T., Kiefer, F., Cassarino, T. G., Bertoni, M., Bordoli, L., and Schwede, T. (2014) SWISS-MODEL: modelling protein tertiary and quaternary structure using evolutionary information. *Nucleic Acids Res. 42*, 252–258.
(48) Cobessi, D., Celia, H., Folschweiller, N., Schalk, I. J., Abdallah, M. A., and Pattus, F. (2005) The crystal structure of the pyoverdine outer membrane receptor fpva from Pseudomonas aeruginosa at 3.6AA Resolution. *J. Mol. Biol. 347*, 121–134.
(49) Correa, N. E., Lauriano, C. M., McGee, R., and Klose, K. E. (2000) Phosphorylation of the flagellar regulatory protein FlrC is necessary for Vibrio cholerae motility and enhanced colonization. *Mol. Microbiol. 35*, 743–755.
(50) Herrero, M., de Lorenzo, V., and Timmis, K. N. (1990) Transposon vectors containing non-antibiotic resistance selection markers for cloning and stable chromosomal insertion of foreign genes in gram-negative bacteria. *J. Bacteriol. 172*, 6557–6567.
(51) Ting, R., Lermer, L., and Perrin, D. M. (2004) Triggering DNAzymes with light: a photoactive c8 thioether-linked adenosine. *J. Am. Chem. Soc. 126*, 12720–12721.